

**CALCULATION OF YOUNG MODULUS OF POLYOLEFIN
NANOCOMPOSITES BY HALPIN TSAI MODEL**

**M.Sc. Thesis by
Özay AKSOY**

Department : Polymer Science and Technology

Programme : Polymer Science and Technology

JANUARY 2011

**CALCULATION OF YOUNG MODULUS OF POLYOLEFIN
NANOCOMPOSITES BY HALPIN TSAI MODEL**

**M.Sc. Thesis by
Özay AKSOY
(515071033)**

**Date of submission : 20 December 2010
Date of defence examination: 25 January 2011**

**Supervisor (Chairman) : Prof. Dr. Nurseli UYANIK (ITU)
Members of the Examining Committee : Prof. Dr. Hulusi ÖZKUL (ITU)
Doç. Dr. Ayfer SARAÇ (YTU)**

JANUARY 2011

İSTANBUL TEKNİK ÜNİVERSİTESİ ★ FEN BİLİMLERİ ENSTİTÜSÜ

**HALPIN TSAI MODELİ KULLANILARAK POLİOLEFİN
NANOKOMPOZİTLERİN YOUNG MODÜLÜNÜN HESAPLANMASI**

**YÜKSEK LİSANS TEZİ
Özay AKSOY
(515071033)**

**Tezin Enstitüye Verildiği Tarih : 20 Aralık 2010
Tezin Savunulduğu Tarih : 25 Ocak 2011**

**Tez Danışmanı : Prof. Dr. Nurseli UYANIK (İTÜ)
Diğer Jüri Üyeleri : Prof. Dr. Hulusi ÖZKUL(İTÜ)
Doç. Dr. Ayfer SARAÇ (YTÜ)**

OCAK 2011

FOREWORD

This study was carried out in Istanbul Technical University, Institute of Science and Technology, Polymer Science and Technology Department.

I would like to express my gratitude to my supervisor Prof. Dr. Nurseli UYANIK who shared her knowledge and experience generously, for her encouragement and supports.

I would like to express my special thanks to Ph.D student Erol Yıldırım to lead to reach the theoretical approach.

I would like to thank to my colleagues in our group and my friends for their support during accomplishment of my MSc study.

I am also grateful to my parents Erdil – Zeynep AKSOY, sister Özgür AKSOY for their great support and understanding throughout preparation of this thesis and accomplishment of courses.

January 2011

Özay Aksoy
Mechanical Engineer
Polymer Science and Technology

TABLE OF CONTENTS

	<u>Page</u>
TABLE OF CONTENTS	vii
ABBREVIATIONS	ix
LIST OF TABLES	xi
LIST OF FIGURES	xiii
SUMMARY	xv
ÖZET	xxi
1. INTRODUCTION	1
2. THEORETICAL PART	3
2.1 Clays	5
2.1.1 Structure and characteristics of layered silicates	5
2.2 Polyethylene	5
2.2.1.1 Low Density Polyethylene (LDPE)	9
2.2.1.2 Linear Low Density Polyethylene (LLDPE).....	10
2.2.1.3 Metallocene Catalysed Polyethylene	10
2.2.2 Structure and properties of Polyethylene	11
2.2.3 Mechanical properties of Polyethylene	13
2.3 Polypropylene.....	16
2.3.1 Structure and properties of Polypropylene.....	20
2.3.2 Mechanical properties of Polypropylene.....	23
2.4 Melt Flow Index	24
2.5 Compatibilizers	25
2.6 Polymer Nanocomposites.....	25
2.6.1 Polymer nanocomposite preparation and synthesis	26
2.6.1.1 Melt intercalation	27
2.6.1.2 Solution dispersion	26
2.6.1.3 In-situ polymerization	28
2.7 Mechanical Properties of Clay-Containing Polypropylene Nanocomposites ..	29
2.8 Composites Theoretical Models for Modeling Elastic Modulus	29
2.8.1 Hui Shia model.....	30
2.8.2 Laminate model.....	30
2.8.3 Modified rule of mixture (MROM).....	31
2.8.4 Mori Tanaka model	32
2.8.5 Halpin Tsai model	32
2.9 Modeling Elastic Modulus of Polymer Layered Silicate Nanocomposites Using a Modified Halpin Tsai Micromechanical Model	33
2.9.1 Effective representation of the nanoclay	36
2.9.1.1 Concept of the effective particle	36
2.9.1.2 Parallel platelet system	38
2.9.1.3 Properties of the effective clay particle	40
3. EXPERIMENTAL PART	43
3.1. Chemical Used	43

3.1.1. Polyethylene, Polypropylene (PE, PP)	43
3.1.1.1 Low Density Polyethylene (LDPE)	43
3.1.1.2 Linear Low Density Polyethylene (LLDPE)	43
3.1.1.1 Metallocene Linear Low Density Polyethylene (mLLDPE)	43
3.1.1.4 Capilene SB56 (Cp)	43
3.1.1.5 Buplen 6531 (Bp)	43
3.1.1.6 Petoplen MH-418 (MH-418)	44
3.1.2 Itaconic Acid (IA).....	44
3.1.3 Montmorillonite (MMT)	44
3.1.3.1 Sodium Montmorillonite (Na-MMT)	44
3.1.3.2 Modified MMT	44
3.1.4 Dodecyl amine (DDA)	44
3.1.5 Hexadecyl amine (HDA).....	45
3.1.6 Octadecyl amine (ODA).....	45
3.2 Preparation of Organoclays	45
3.3 Preparation of Polymer Nanocomposites	45
3.4 Calculation Process Using Modified Halpin Tsai Micromechanical Modeling.....	46
3.5 Calculations Using Modified Halpin Tsai Micromechanical Modeling	47
3.5.1 Calculation of “ l/t ”	47
3.5.1.1 MRF	47
3.5.1.2 Young' modulus of polymeric nanocomposites (E_c)	47
3.5.1.3 Young modulus of pure polymers (E_m)	49
3.5.1.4 Young Modulus of montmorillonite (E_f)	49
3.5.1.5 MMT content in organoclays and filler volume fraction (Φ_f)	49
3.5.1.6 Density of clay	52
3.5.1.7 Density of pure polymers	53
3.5.1.8 Densities of used organoclays	53
3.5.1.9 Densities of compatibilizers	53
3.5.2 Calculated values “ l/t ”	53
4. CONCLUSION AND RECOMMENDATIONS	55
4.1 Calculation of “ l/t ” Values of Experimental Young Modulus Data	55
4.2 Calculation of Young Modulus Values of Different Types of Nanocomposites by Halpin Tsai Micromechanical Model	58
REFERENCES	61
CURRICULUM VITAE.....	65

ABBREVIATIONS

OC	: Organoclay
COM	: Compatibilizer
IO	: Inorganic
PNC	: Polymeric Nanocomposite
PP	: Polypropylene
Cp	: Capilene Polypropylene
Bp	: Buplen Polypropylene
MH-418	: Petoplen MH-418 Polypropylene
PPNC	: Polypropylene Nanocomposite
PO	: Polyolefine
PE	: Polyethylene
NC	: Nanocomposite
PNC	: Polymer Nanocomposites
LDPE	: Low Density Polyethylene
LLDPE	: Linear Low Density Polyethylene
mLLDPE	: Metallocene Linear Low Density Polyethylene
IA	: Itaconic Acid
MMT	: Montmorillonite
NIISRT	: Notched Izod Impact Strength

LIST OF TABLES

	<u>Page</u>
Table 2.1: Chemical structure of commonly used 2:1 phyllosilicates	7
Table 2.2: Comparison of Blown Film Properties of LLDPE and LDPE.....	10
Table 2.3: Crystallinity data for polyethylene.....	12
Table 2.4: Effect of straining rate on the measured tensile strength and elongation at break of two samples of polyethyleneOne-line table title with centred columns	15
Table 2.5: Some mechanical and thermal properties of commercial polypropylenes	22
Table 2.6: Characteristic values of the polymer-clay structure – descriptive parameters	37
Table 3.1: Young modulus of used polymer nanocomposites	47
Table 3.2: Young modulus of used pure polymers	49
Table 3.3: MMT contents of organoclay used in this work	50
Table 3.4: Calculated filler volume fraction of the samples	51
Table 3.5: Densities of pure polymers	52
Table 3.6: Densities of used organoclays.....	53
Table 3.7: Calculated “ l/t ” values of samples	54
Table 4.1: Calculated “ l/t ” values below 10.....	56
Table 4.2: Calculated “ l/t ” values between 10 and 50	56
Table 4.3: Calculated “ l/t ” values between 50 and 100	57
Table 4.4: Calculated “ l/t ” values upper than 100	57

LIST OF FIGURES

	<u>Page</u>
Figure 2.1 : Nomenclature of polymeric nanocomposites.....	4
Figure 2.2 : Structure of a 2:1 layered silicate.....	7
Figure 2.3 : Chain configurations of polyethylene.....	9
Figure 2.4 : Polymerization of PE.....	9
Figure 2.5 : Polyethylene structure	11
Figure 2.6 : Effect of polymer density, testing rate and temperature on the shape of the stress-strain curve for polyethylene. Single linkage distance.	14
Figure 2.7 : Effect of temperature on the tensile stress-strain for polyethylene. (Low-density polymer $\sim 0.92 \text{ g/cm}^3$, MFI=2.) Rate of extension 190% per minute.	16
Figure 2.8 : Isotactic, syndiotactic, and atactic polymer chains.	17
Figure 2.9 : Polymerization of Polypropylene	17
Figure 2.10 : Effect of isotacticity on tensile properties.	21
Figure 2.11 : Schematic representation of the dispersion process of the organized clay in the PP matrix with the aid of PP-g-MAH.	26
Figure 2.12 : Schematic depicting the intercalation process between a polymer melt and an organically modified layered silicate.	28
Figure 2.13 : Method for creating intercalated polymer-clay architectures via direct polymer contact and via in-situ polymerization of pre intercalated polymers.	29
Figure 2.14 : Schematic illustrations of types of polymer/clay composites.	35
Figure 2.15 : Schematic of the polymer-clay morphology and characteristic parameters.....	38
Figure 2.16 : Simplified schematic showing (L to R) an individual clay platelet, a compact clay tactoid, and a swollen clay tactoid.....	39
Figure 2.17 : A representative element of an intercalated cluster of clay nanolayers assumptions as a parallel platelet system	39
Figure 2.18 : Dependence of particle silicate volume fraction X on clay structural parameters N and $d_{(001)}/d_s$	40
Figure 3.1 : TGA curves of natural and organomodified montmorillonites with various concentrations of hexadecylamine (related to the clay CEC).	49
Figure 3.2 : Dependence of particle silicate volume fraction X on clay structural parameters N and $d_{(001)}/d_s$	40
Figure 4.1 : Composite modulus versus nanofil 8 content graph of LDPE	58
Figure 4.2 : Composite modulus versus nanofil 8 content graph of LLDPE.....	59
Figure 4.3 : Composite modulus versus nanofil 8 content graph of PP (Buplen)...	60

CALCULATION OF YOUNG MODULUS OF POLYOLEFINS BY HALPIN TSAI MODEL

SUMMARY

Polyolefins (PO) are the most widely used polymers. It is often compounded with natural minerals to enhance its stiffness, toughness, dimensional-stability, and some other properties. Nowadays, preparation of nanocomposites is widely used to improve the the properties. Nanocomposites (NCs) are a combination of two or more phases containing different compositions, where at least one of the phases is in the nanoscale regime. Preparation of PO-based polymer / (organo) clay nanocomposites (PNC) is more difficult than other polymers, which contains polar groups in its backbone. Homogeneous dispersion of polar clay cannot be realized due to lack of PO miscibility with organically-modified clay (organoclay). Strong interaction between a non-polar polymer (e.g. PO) and polar organoclay might be achieved with addition of a compatibilizer. The convenient way of preparing a compatibilizer is polar functionalization of the original PO.

The properties of the composites are determined by those of the components, shape, and volume fraction of the filler as well as by the morphology of the system and the nature of the interphase that sometimes develop at the interface of the components. Although there is no direct correlation between the filler particle size and the composite properties. The aspect ratio of the inclusions also strongly influences the tensile properties. Generally, the elastic modulus increases with the filler volume fraction, while all other tensile properties such as the yield stress and strain, the ultimate stress, and strain almost invariably decrease with increasing filler volume fraction. Models developed to predict the modulus of composites are mainly based on either hydrodynamic considerations or on continuum solid mechanics and its modifications such as Halpin Tsai.

In this study, Halpin Tsai model was chosen to examine aspect ratio (l/t) of polyolefin nanocomposites by using the measured values of Young's modulus of PO NCs. The values were obtained from the experimental results. The used parameters in these approach are Young's modulus of pure matrix (PO) and filler (clay); mass and density of ingredients, nanoparticles and organoclays. Modulus Reduction Factor (MRF) was included in modified model for platelet type nanoparticles. The advantage of Halpin Tsai model is that it can be applied to many systems including different type of matrix material and filler types. Tactoid model (stack of nanoparticles) was developed for polymer nanocomposites for examining properties. The data used in this study belongs to experimental results based on previously developed various polyethylene and polypropylene nanocomposites; and other universal values obtained from literature.

Halpin Tsai micromechanical model is a well-known composites theory in the fibre composites industry to examine elastic moduli of unidirectional composites as the function of filler volume fraction and aspect ratio. In this model, filler geometries can

be different with discontinuous reinforcements such as fibre-like or flake-like fillers. The longitudinal and transverse moduli of a composite material in Halpin Tsai model are generally expressed as

$$\frac{E_c}{E_m} = \frac{1 + \zeta \eta \phi_f}{1 - \eta \phi_f} \quad \eta = \frac{\left(\frac{E_f}{E_m}\right) - 1}{\left(\frac{E_f}{E_m}\right) + \zeta} \quad (1) \quad (2)$$

where “ E_c ”, “ E_f ” and “ E_m ” are Young’s moduli of composites, fillers and the polymer matrix, respectively. “ ϕ_f ” is the filler volume fraction and “ ζ ” is a shape parameter depending on the filler geometry and loading direction. “ $\zeta = 2(l/t)$ ” for “ l ” and “ t ”, are the length and thickness of dispersed fillers, respectively.

The used polyethylene data are belonging to low density polyethylene (LDPE), linear low density polyethylene (LLDPE), metallocene linear low density polyethylene (mLLDPE). The isotactic polypropylenes used to calculate “ l/t ” ratios are Capilene, Buplene, and MH-418.

MRF, E_c , E_m , E_f , Φ_f , density of montmorillonite- pure polymers- organoclays are used to calculate “ l/t ” by using Halpin Tsai approach.

Initially, Φ_f (filler volume fraction) is calculated from density and mass of ingredients of polymeric nanocomposites. Since montmorillonite is used as fillers in Halpin Tsai approach, filler volume fraction can be calculated with the help of TGA analysis of ingredients. Montmorillonite content of organoclays was obtained from TGA analysis. Density of compatibilizers are used same with pure polymer matrixes.

Firstly, organoclay mass is divided by MMT density. In order to calculate volume of montmorillonite content, result is multiplied by MMT weight percentage data that can be obtained from TGA analysis.

Secondly, total volume of nanocomposite is calculated by summing volume of each ingredient by dividing mass over density.

Thirdly, volume of montmorillonite is divided by total volume, from which Φ_f (filler volume fraction) is obtained.

The equation for calculation of filler volume fraction (Φ_f) is given as follows:

$$\phi_f = \frac{\left(\frac{\text{Mass of Organoclay} * \text{MMT Content}}{\text{Density of MMT Content}}\right)}{\left(\frac{\text{Mass of organoclay}}{\text{Density of organoclay}}\right) + \left(\frac{\text{Mass of Compatibilizer}}{\text{Density of Compatibilizer}}\right) + \left(\frac{\text{Mass of polymer matrix}}{\text{Density of polymer matrix}}\right)} \quad (3)$$

Table 1: Calculated filler volume fraction of the samples

Polymeric Nanocomposites	Φ_f –Filler Volume Fraction	Organo-Clay Content (%)	Compa-tibilizer Content (%)	Polymer Matrix Content (%)
LDPE-IA-O _{DDA} 5-C5	0.011062035	5	5	90
LDPE-IA-O _{DDA} 5-C10	0.011062035	5	10	85
LDPE-IA-O _{DDA} 5-C15	0.011062035	5	15	80
LDPE- MMI-O _{DDA} 5-C5	0.011062035	5	5	90
LDPE- MMI-O _{DDA} 5-C10	0.011062035	5	10	85
LDPE- MMI-O _{DDA} 5-C15	0.011062035	5	15	80
LDPE-IA-O _{HDA} 5-C5	0.014079687	5	5	90

LDPE-IA-O _{HDA} 5-C10	0.014079687	5	10	85
LDPE-IA-O _{HDA} 5-C15	0.014079687	5	15	80
LDPE- MMI-O _{HDA} 5-C5	0.014079687	5	5	90
LDPE- MMI-O _{HDA} 5-C10	0.014079687	5	10	85
LDPE- MMI-O _{HDA} 5-C15	0.014079687	5	15	80
LDPE-IA-O _{ODA} 5-C5	0.013179744	5	5	90
LDPE-IA-O _{ODA} 5-C10	0.013179744	5	10	85
LDPE-IA-O _{ODA} 5-C15	0.013179744	5	15	80
LDPE- MMI-O _{ODA} 5-C5	0.013179744	5	5	90
LDPE- MMI-O _{ODA} 5-C10	0.013179744	5	10	85
LDPE- MMI-OC _{ODA} 5-C15	0.013179744	5	15	80
LLDPE-IA-O _{DDA} 5-C5	0.011085363	5	5	90
LLDPE-IA-O _{DDA} 5-C10	0.011085363	5	10	85
LLDPE-IA-O _{DDA} 5-C15	0.011085363	5	15	80
LLDPE-MMI-O _{DDA} 5-C5	0.011085363	5	5	90
LLDPE-MMI-O _{DDA} 5-C10	0.011085363	5	10	85
LLDPE-MMI-O _{DDA} 5-C15	0.011085363	5	15	80
LLDPE-IA-O _{HDA} 5-C5	0.014109346	5	5	90
LLDPE-IA-O _{HDA} 5-C10	0.014109346	5	10	85
LLDPE-IA-O _{HDA} 5-C15	0.014109346	5	15	80
LLDPE-MMI-O _{HDA} 5-C5	0.014109346	5	5	90
LLDPE-MMI-O _{HDA} 5-C10	0.014109346	5	10	85
LLDPE-MMI-O _{HDA} 5-C15	0.014109346	5	15	80
LLDPE-IA-O _{ODA} 5-C5	0.013207489	5	5	90
LLDPE-IA-O _{ODA} 5-C10	0.013207489	5	10	85
LLDPE-IA-O _{ODA} 5-C15	0.013207489	5	15	80
LLDPE-MMI-O _{ODA} 5-C5	0.013207489	5	5	90
LLDPE-MMI-O _{ODA} 5-C10	0.013207489	5	10	85
LLDPE-MMI-O _{ODA} 5-C15	0.013207489	5	15	80
mLLDPE- O _{ODA} 5 - C 5	0.013235230	5	5	90
mLLDPE - O _{ODA} 5 - C 10	0.013235230	5	10	85
mLLDPE - O _{ODA} 5 - C 15	0.013235230	5	15	80
mLLDPE - O _{ODA} 5 - C 20	0.013235230	5	20	75
PP _{CAP} - O _{NANOFIL8} 3 - C10	0.005920595	3	10	87
PP _{CAP} - O _{NANOFIL8} 5-C15	0.009959508	5	15	80
PP _{BUP} - O _{NANOFIL8} 3- C10	0.005894859	3	10	87
PP _{BUP} - O _{NANOFIL8} 5- C15	0.009916710	5	15	80
PP _{MH418} - O _{NANOFIL8} 3- C10	0.005920595	3	10	87
PP _{MH418} - O _{NANOFIL8} 5- C 15	0.009959508	5	15	80

Table 2: Densities of pure polymers

Polymer	Density (kg/m ³)
LDPE	923
LLDPE	925
mLLDPE	927
Capilene SB56	901
Buplen 6531	905
Petoplen MH-418	905

Table 3: Densities of used organoclays

Organoclay	Density (kg/m ³)
MMT - DDA	1770
MMT - HDA	1700
MMT - ODA	1660
Nanofil 8	1660

In Halpin Tsai equations $\zeta = 2(l/t)$, “ l/t ” is length over thickness ratio of tactoids, we can derive intercalated or exfoliated structure from these data.

Table 4.1: “ l/t ” values of LDPE

Polymeric nanocomposites	l/t
LDPE-IA-O _{DDA} 5-C5	0.47
LDPE-IA-O _{DDA} 5-C10	51.86
LDPE-IA-O _{DDA} 5-C15	54.59
LDPE- MMI-O _{DDA} 5-C5	31.73
LDPE- MMI-O _{DDA} 5-C10	57.09
LDPE- MMI-O _{DDA} 5-C15	82.82
LDPE-IA-O _{HDA} 5-C5	55.97
LDPE-IA-O _{HDA} 5-C10	83.11
LDPE-IA-O _{HDA} 5-C15	128.18
LDPE- MMI-O _{HDA} 5-C5	44.44
LDPE- MMI-O _{HDA} 5-C10	67.12
LDPE- MMI-O _{HDA} 5-C15	115.88
LDPE-IA-O _{ODA} 5-C5	42.09
LDPE-IA-O _{ODA} 5-C10	65.76
LDPE-IA-O _{ODA} 5-C15	82.94
LDPE- MMI-O _{ODA} 5-C5	30.35
LDPE- MMI-O _{ODA} 5-C10	48.04
LDPE- MMI-OC _{ODA} 5-C15	67.94

Table 4.2: “ l/t ” values of LLDPE

Polymeric nancomposites	l/t
LLDPE-IA-O _{DDA} 5-C5	31.55
LLDPE-IA-O _{DDA} 5-C10	56.93
LLDPE-IA-O _{DDA} 5-C15	67.52
LLDPE- MMI-O _{DDA} 5-C5	26.10
LLDPE- MMI-O _{DDA} 5-C10	42.90
LLDPE- MMI-O _{DDA} 5-C15	63.23
LLDPE-IA-O _{HDA} 5-C5	26.91
LLDPE-IA-O _{HDA} 5-C10	40.92
LLDPE-IA-O _{HDA} 5-C15	50.79
LLDPE- MMI-O _{HDA} 5-C5	22.83
LLDPE- MMI-O _{HDA} 5-C10	37.92
LLDPE- MMI-O _{HDA} 5-C15	49.22
LLDPE-IA-O _{ODA} 5-C5	13.13
LLDPE-IA-O _{ODA} 5-C10	50.44
LLDPE-IA-O _{ODA} 5-C15	99.48
LLDPE- MMI-O _{ODA} 5-C5	13.13
LLDPE- MMI-O _{ODA} 5-C10	38.32
LLDPE- MMI-O _{ODA} 5-C15	100.31

Table 4.3: “ l/t ” values of samples mLLDPE , PP

Polymeric nancomposites	l/t
mLLDPE- O _{ODA} 5 - C 5	7.72
mLLDPE - O _{ODA} 5 - C 10	8.43
mLLDPE - O _{ODA} 5 - C 15	0.34
mLLDPE - O _{ODA} 5 - C 20	0.01
PP _{CAP} - O _{NANOFIL8} 3 - C10	0.01
PP _{CAP} - O _{NANOFIL8} 5-C15	18.31
PP _{BUP} - O _{NANOFIL8} 3- C10	37.41
PP _{BUP} - O _{NANOFIL8} 5- C15	30.54
PP _{MH418} - O _{NANOFIL8} 3- C10	11.03
PP _{MH418} - O _{NANOFIL8} 5- C 15	11.77

In some calculation, the intercalation can be obtained either experimental XRD results or Halpin Tsai approach “ l/t ” calculations. The experimental XRD results which give the d-spacing and the calculated “ l/t ” of the POs give a presumption of nanocomposite structure. The results calculated “ l/t ” by Halpin Tsai models consistent for the experimental XRD values. (Table 4.1, Table 4.2, Table 4.3)

For some samples partial exfoliation leads to an appreciable increase in the elastic modulus of the nanocomposites and “ l/t ” values are higher than 100 for the samples while the complete exfoliation approaches to 200 depending on the aspect ratio of clay.

In graphs below, “ l/t ” values are taken as 10, 50, 100, 200 respectively in Halpin Tsai formulas. LDPE, LLDPE, PP (Buplen); Nanofil 8 are used and their properties are taken from section 3. %1, %5, %10 Nanofil 8 content are used in calculations, and mass of taken compatibilizers are three times of organoclay content. Following figures are obtained.

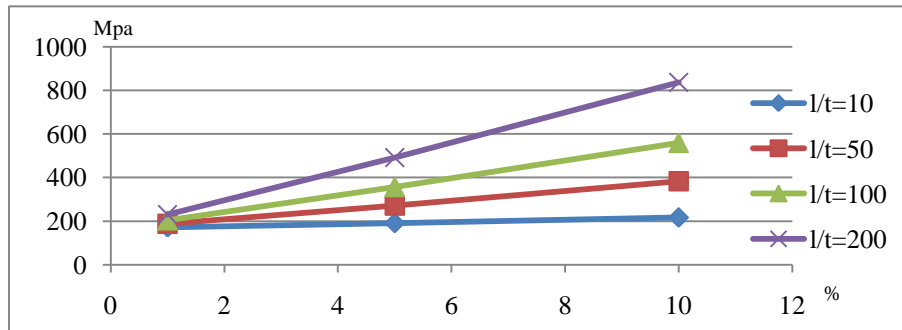


Figure 1 : Composite modulus versus Nanofil 8 content graph of LDPE

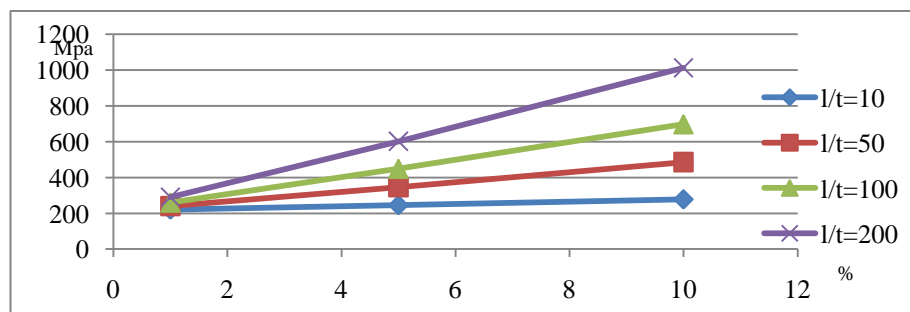


Figure 2 : Composite modulus versus Nanofil 8 content graph of LLDPE

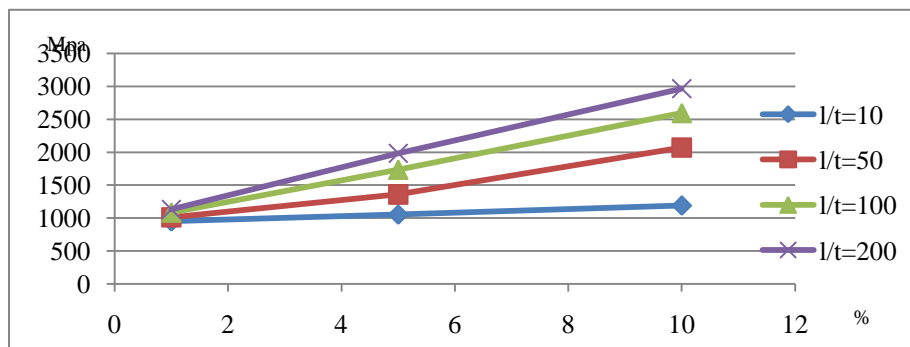


Figure 3 : Composite modulus versus Nanofil 8 content graph of PP (Buplen)

In above graphs “ l/t ” ratios change from 10 to 200. As “ l/t ” ratio rises, dispersion of layers increases in structure. This causes increment in Young modulus of polymeric nanocomposite. The higher content of organoclay, the higher elastic modulus of PNC.

It was observed that in graphs that, the slope of lines differ each other because of Young’s modulus differences of LDPE, LLDPE, PP (Buplen).

HALPIN TSAI MODELİ KULLANILARAK POLİOLEFİNLERİN YOUNG MODÜLÜNÜN HESAPLANMASI

ÖZET

Poliiolefinler en yaygın kullanılan polimerlerdir. Poliiolefinler, elastisite modülü, tokluk, boyutsal kararlılık ve diğer özelliklerinin arttırılması için doğal minerallerle karıştırılır. Nanokompozitler bu bağlamda yaygın olarak kullanılmaktadır, polimerik nanokompozitler farklı bileşenlere sahip farklı iki fazın toplamından oluşmaktadır ve bu fazlardan en az biri nano ölçektedir. Poliiolefin matriksli organokil içeren nanokompozitlerin hazırlanması, ana zincirinde polar grup taşıyan diğer polimerlere nazaran daha zordur. Polar kilin homojen olarak dağılması, poliiolefin ve organik olarak modifiye edilmiş kilin karıştırılmaması nedeniyle gerçekleştirilemez. Polar olmayan polimer ve polar organokil arasındaki güçlü etkileşim ancak uyumlaştırıcı katılmasıyla mümkün olabilir. Uyumlaştırıcı hazırlanmasına en uygun yöntem, orjinal poliiolefinlerin polar fonksiyonlaştırılmasıdır.

Kompozitlerin özellikleri, dolgu malzemesinin hacmi ve boy-kalınlık oranı, sistemin yapısı ve bazen alt bileşenler arası etkileşimi oluşturan arafazın doğası ile ilişkilidir. Kompozit özellikleri ve dolgu parçacık boyutu arasında doğrudan bir ilişki bulunmamasına rağmen, taneciklerin uzunluğunun kalınlığına oranı dayanım özelliklerini baskın bir şekilde etkilemektedir. Genel olarak, elastik modülü taneciklerin dolgu oranı ile artmaktadır fakat çekme dayanımı ve uzaması, maksimum gerilme ve uzaması artan tanecik dolgu oranı ile azalmaktadır. Kompozitlerin Young modüllerini öngörmek için geliştirilen modellerde, ya hidrodinamik yaklaşımlar ya da sürekli ortamlar mekaniği ve türevleri temel alınmıştır.

Bu çalışmada poliiolefin nanokompozitlerde bulunan partiküllerin uzunluğunun kalınlığına oranını (l/t) öngörmek için Halpin Tsai modeli seçilmiştir. Poliiolefinlerin Young modülleri deneysel değerlerden elde edilmiştir. Hesaplamalarda kullanılan parametreler, polimer matriksin ve kilin Young modülü, bileşenlerin-nanopartiküllerin - organokillerin kütle ve yoğunluklarıdır. Modül etkisini azaltma oranı (MRF) tabakalı nanotanecikler için hesaba katılmıştır. Halpin Tsai modelinin avantajı çok farklı matriks malzemesi ve katkı tiplerine uygulanabilir olmasıdır. Halpin Tsai yaklaşımındaki taktoit model (nanopartiküllerin matris içindeki dağılımı), nanokompozitlerin özelliklerini incelemek için geliştirilmiştir. Bu çalışmada kullanılmış olan veriler, daha önceden geliştirilmiş olan polietilen ve polipropilen örneklerin deneysel sonuçları ve literatür incelemelerinden elde edilmiştir.

Halpin Tsai mikromekanik modeli, katkı hacmi ve boy-kalınlık oranı yardımıyla tek yönlü kompozitlerin elastik modülünün incelenmesinde kullanılan, fiber kompozit endüstrisinde yaygın olarak bilinen bir kompozit teorisidir. Bu modelde dolgu geometrileri elyaf ya da tabakalı yapı gibi farklı geometrilere süreksiz bir biçimde

olabilir. Halpin Tsai yaklaşımında kompozit malzemenin elastisite modülü hesaplaması aşağıdaki gibi özetlenebilir.

$$\frac{E_c}{E_m} = \frac{1 + \zeta \eta \phi_f}{1 - \eta \phi_f} \quad \eta = \frac{\left(\frac{E_f}{E_m}\right) - 1}{\left(\frac{E_f}{E_m}\right) + \zeta} \quad (1)(2)$$

“ E_c ”, “ E_f ” and “ E_m ” sırasıyla kompozit, dolgu malzemesi ve polimer matriksin Young modülleridir. “ ϕ_f ”, dolgu malzemesinin hacim oranıdır. “ ζ ” dolgu geometrisi ve yükleme oranına bağlı bir boyut parametresidir. “ $\zeta = 2(l/t)$ ” formülünde sırasıyla “ l ” ve “ t ”, dağılmış olan dolguların boy ve kalınlıklarıdır.

Kullanılan polietilen verileri alçak yoğunluklu polietilen (AYPE), doğrusal alçak yoğunluklu polietilen (DAYPE), metalosen doğrusal alçak yoğunluklu polietilen (mDAYPE) verilerine aittir. “ l/t ” oranlarını hesaplamak için kullanılan polipropilenler Capilene, Buplene ve MH-418’dir.

MRF, E_c , E_m , E_f , ϕ_f ; montmorillonit, saf polimer ve organokil yoğunluklarını kullanarak Halpin Tsai yaklaşımındaki “ l/t ” oranlarını hesaplandı.

ϕ_f (katkının hacim oranı), polimerik nanokompozit bileşenlerinin kütle ve hacimlerinden hesaplanır. Bu yaklaşımda montmorillonit katkı maddesi olarak kabul edildiği için katkı hacim oranı bileşenlerin TGA analizinden elde edilir. TGA analizinden organokilde bulunan MMT içeriği belirlenir. Uyumlaştırıcıların yoğunlukları saf polimerlerle aynı kabul edilmiştir.

İlk olarak organokilin kütlelerini MMT yoğunluğuna bölünür. Montmorillonit içeriğinin hacmini hesaplamak için sonuç, TGA verilerinden elde edilen yüzdelik MMT ağırlık oranı ile çarpılır.

İkinci olarak, bileşenlerin kütlelerini hacimlerine bölerek nanokompozitin toplam hacmi elde edilir.

Üçüncü olarak, montmorillonit hacmi toplam hacme bölünür, sonuç olarak ϕ_f (katkının hacim oranı) elde edilir.

Katkının hacim oranı denklemi (ϕ_f) aşağıdaki gibidir:

$$\phi_f = \frac{\left(\frac{\text{Organokil Kütlesi} * \text{MMT İçeriği}}{\text{MMT İçeriğinin Yoğunluğu}}\right)}{\left(\frac{\text{Organokil Kütlesi}}{\text{Organokil Yoğunluğu}}\right) + \left(\frac{\text{Uyumlaştırıcı Kütlesi}}{\text{Uyumlaştırıcı Yoğunluğu}}\right) + \left(\frac{\text{Polimer Matriks Kütlesi}}{\text{Polimer Matriks Yoğunluğu}}\right)} \quad (3)$$

Tablo 1: Örneklerde hesaplanan katkı hacim oranları

Polimerik Nanokompozitler	ϕ_f -Katkı Hacim Oranı	Organo-Kil İçeriği (%)	Uyumlaştırıcı İçeriği (%)	Polimer Matriks İçeriği (%)
AYPE-IA-O _{DDA} 5-C5	0.011062035	5	5	90
AYPE-IA-O _{DDA} 5-C10	0.011062035	5	10	85
AYPE-IA-O _{DDA} 5-C15	0.011062035	5	15	80
AYPE- MMI-O _{DDA} 5-C5	0.011062035	5	5	90
AYPE- MMI-O _{DDA} 5-C10	0.011062035	5	10	85
AYPE- MMI-O _{DDA} 5-C15	0.011062035	5	15	80
AYPE-IA-O _{HDA} 5-C5	0.014079687	5	5	90

AYPE-IA-O _{HDA} 5-C10	0.014079687	5	10	85
AYPE-IA-O _{HDA} 5-C15	0.014079687	5	15	80
AYPE- MMI-O _{HDA} 5-C5	0.014079687	5	5	90
AYPE- MMI-O _{HDA} 5-C10	0.014079687	5	10	85
AYPE- MMI-O _{HDA} 5-C15	0.014079687	5	15	80
AYPE-IA-O _{ODA} 5-C5	0.013179744	5	5	90
AYPE-IA-O _{ODA} 5-C10	0.013179744	5	10	85
AYPE-IA-O _{ODA} 5-C15	0.013179744	5	15	80
AYPE- MMI-O _{ODA} 5-C5	0.013179744	5	5	90
AYPE- MMI-O _{ODA} 5-C10	0.013179744	5	10	85
AYPE- MMI-O _{ODA} 5-C15	0.013179744	5	15	80
DAYPE-IA-O _{DDA} 5-C5	0.011085363	5	5	90
DAYPE-IA-O _{DDA} 5-C10	0.011085363	5	10	85
DAYPE-IA-O _{DDA} 5-C15	0.011085363	5	15	80
DAYPE-MMI-O _{DDA} 5-C5	0.011085363	5	5	90
DAYPE-MMI-O _{DDA} 5-C10	0.011085363	5	10	85
DAYPE-MMI-O _{DDA} 5-C15	0.011085363	5	15	80
DAYPE-IA-O _{HDA} 5-C5	0.014109346	5	5	90
DAYPE-IA-O _{HDA} 5-C10	0.014109346	5	10	85
DAYPE-IA-O _{HDA} 5-C15	0.014109346	5	15	80
DAYPE-MMI-O _{HDA} 5-C5	0.014109346	5	5	90
DAYPE-MMI-O _{HDA} 5-C10	0.014109346	5	10	85
DAYPE-MMI-O _{HDA} 5-C15	0.014109346	5	15	80
DAYPE-IA-O _{ODA} 5-C5	0.013207489	5	5	90
DAYPE-IA-O _{ODA} 5-C10	0.013207489	5	10	85
DAYPE-IA-O _{ODA} 5-C15	0.013207489	5	15	80
DAYPE-MMI-O _{ODA} 5-C5	0.013207489	5	5	90
DAYPE-MMI-O _{ODA} 5-C10	0.013207489	5	10	85
DAYPE-MMI-O _{ODA} 5-C15	0.013207489	5	15	80
mDAYPE- O _{ODA} 5 - C 5	0.013235230	5	5	90
mDAYPE - O _{ODA} 5 - C 10	0.013235230	5	10	85
mDAYPE - O _{ODA} 5 - C 15	0.013235230	5	15	80
mDAYPE - O _{ODA} 5 - C 20	0.013235230	5	20	75
PP _{CAP} - O _{NANOFIL8} 3 - C10	0.005920595	3	10	87
PP _{CAP} - O _{NANOFIL8} 5-C15	0.009959508	5	15	80
PP _{BUP} - O _{NANOFIL8} 3- C10	0.005894859	3	10	87
PP _{BUP} - O _{NANOFIL8} 5- C15	0.009916710	5	15	80
PP _{MH418} - O _{NANOFIL8} 3- C10	0.005920595	3	10	87
PP _{MH418} - O _{NANOFIL8} 5- C 15	0.009959508	5	15	80

Tablo 2: Saf polimerlerin yoğunlukları

Polimer	Yoğunluk (kg/m ³)
AYPE	923
DAYPE	925
mDAYPE	927
Capilene SB56	901
Buplen 6531	905
Petoplen MH-418	905

Tablo 3: Organokillerin yoğunlukları

Organokil	Yoğunluk (kg/m ³)
MMT - DDA	1770
MMT - HDA	1700
MMT - ODA	1660
Nanofil 8	1660

Halpin Tsai denklemlerinde $\zeta = 2(l/t)$ kullanılmaktadır, bu yaklaşımda kil tabakalarının “ l/t ” değerlerini inceleyerek, polimer nanokompozit içindeki oluşumunun sıralı tabakalı (intercalated) dağıtılmış tabakalı (exfoliated) olduğu belirlenebilir.

Tablo 4.1: “ l/t ” değerleri AYPE

Polimerik Nanokompozitler	l/t
AYPE-IA-O _{DDA} 5-C5	0.46
AYPE-IA-O _{DDA} 5-C10	51.85
AYPE-IA-O _{DDA} 5-C15	54.59
AYPE- MMI-O _{DDA} 5-C5	31.73
AYPE- MMI-O _{DDA} 5-C10	57.09
AYPE- MMI-O _{DDA} 5-C15	82.82
AYPE-IA-O _{HDA} 5-C5	55.97
AYPE-IA-O _{HDA} 5-C10	83.11
AYPE-IA-O _{HDA} 5-C15	128.18
AYPE- MMI-O _{HDA} 5-C5	44.44
AYPE- MMI-O _{HDA} 5-C10	67.12
AYPE- MMI-O _{HDA} 5-C15	115.88
AYPE-IA-O _{ODA} 5-C5	42.09
AYPE-IA-O _{ODA} 5-C10	65.76
AYPE-IA-O _{ODA} 5-C15	82.94
AYPE- MMI-O _{ODA} 5-C5	30.35
AYPE- MMI-O _{ODA} 5-C10	48.04
AYPE- MMI-O _{ODA} 5-C15	67.94

Tablo 4.2: “ l/t ” değerleri DAYPE

Polimerik Nanokompozitler	l/t
DAYPE-IA-O _{DDA} 5-C5	31.55
DAYPE-IA-O _{DDA} 5-C10	56.93
DAYPE-IA-O _{DDA} 5-C15	67.52
DAYPE-MMI-O _{DDA} 5-C5	26.10
DAYPE-MMI-O _{DDA} 5-C10	42.90
DAYPE-MMI-O _{DDA} 5-C15	63.23
DAYPE-IA-O _{HDA} 5-C5	26.91
DAYPE-IA-O _{HDA} 5-C10	40.92
DAYPE-IA-O _{HDA} 5-C15	50.79
DAYPE-MMI-O _{HDA} 5-C5	22.83
DAYPE-MMI-O _{HDA} 5-C10	37.92
DAYPE-MMI-O _{HDA} 5-C15	49.22
DAYPE-IA-O _{ODA} 5-C5	13.13
DAYPE-IA-O _{ODA} 5-C10	50.44
DAYPE-IA-O _{ODA} 5-C15	99.48
DAYPE-MMI-O _{ODA} 5-C5	13.13
DAYPE-MMI-O _{ODA} 5-C10	38.32
DAYPE-MMI-O _{ODA} 5-C15	100.31

Table 4.3: “ l/t ” değerleri mLLDPE , PP

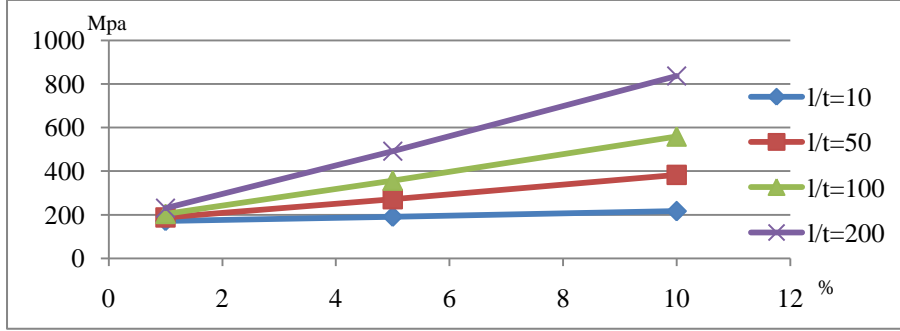
Polimerik Nanokompozitler	l/t
mDAYPE- O _{ODA} 5 - C 5	7.72
mDAYPE - O _{ODA} 5 - C 10	8.43
mDAYPE - O _{ODA} 5 - C 15	0.34
mDAYPE - O _{ODA} 5 - C 20	0.01
PP _{CAP} - O _{NANOFIL8} 3 - C10	0.01
PP _{CAP} - O _{NANOFIL8} 5-C15	18.31
PP _{BUP} - O _{NANOFIL8} 3- C10	37.41
PP _{BUP} - O _{NANOFIL8} 5- C15	30.54
PP _{MH418} - O _{NANOFIL8} 3- C10	11.03
PP _{MH418} - O _{NANOFIL8} 5- C 15	11.77

Nanopartiküllerin yapısı, XRD sonuçlarında ya da Halpin Tsai yaklaşımıyla elde edilen “ l/t ” değerleriyle incelenebilir. d -aralıklarını veren deneysel XRD sonuçları ve hesaplanan “ l/t ” değerleri poliolefin nanokompozit yapısı hakkında ipucu verir.

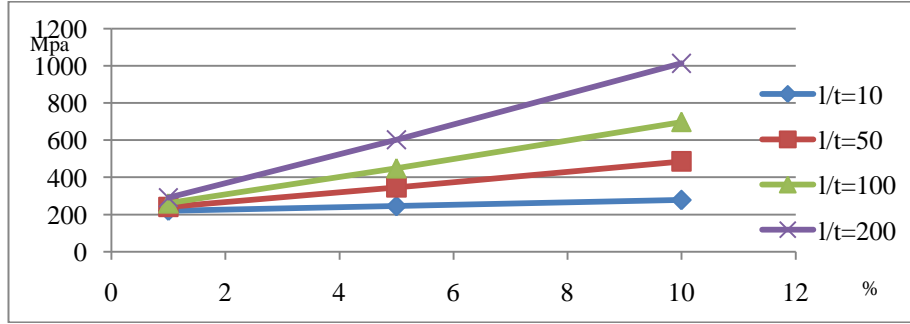
Bu çalışmada Halpin Tsai modeli yardımıyla hesaplanan “ l/t ” değerleri, XRD değerleriyle uyumludur.(Tablo 4.1, Tablo 4.2, Tablo 4.3)Yapılan çalışmada örneklerin 50-100 arasında hesaplanan “ l/t ” değerleri sıralı tabakalı (intercalated) nanokompozit yapısını göstermektedir. Bazı örnekler için kısmi dağıtılmış tabakalı (exfoliated) nanokompozit yapısı elastik modülde belirginbir artış gösterir ve bu örneklerde “ l/t ” değerleri 100’den yüksek çıkmıştır.

Tam dağıtılmış tabakalı (exfoliated) nanokompozit yapısı durumunda beklenen “ l/t ” değerleri kilin uzunluk/kalınlık oranına bağlı olarak 200 civarında beklenebilir.

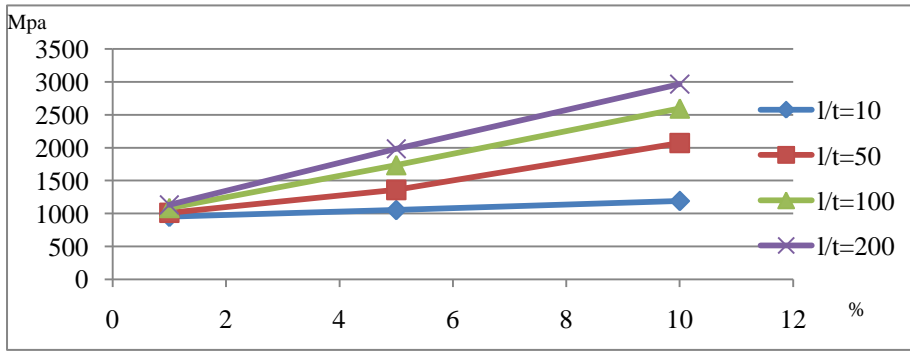
Aşağıdaki grafiklerde görüldüğü gibi, Halpin Tsai denklemlerindeki “ l/t ” değerleri sırasıyla 10, 50, 100, 200 alınmıştır. LDPE, LLDPE, PP (Buplen); Nanofil 8 kullanılmış olup, özellikleri Bölüm 3’ten alınmıştır. Hesaplamalarda %1, %5, %10 Nanofil 8 içeriği kullanılmıştır ve kullanılan uyumlaştırıcıların miktarı, organokil içeriğinin üç katıdır. Aşağıdaki şekiller elde edilmiştir.



Şekil 1 : Kompozit modülü, Nanofil 8 içerik grafiği - AYPE



Şekil 2 : Kompozit modülü, Nanofil 8 içerik grafiği - DAYPE



Şekil 3 : Kompozit modülü, Nanofil 8 içerik grafiği - PP (Buplen)

Yukarıdaki grafiklerde “ l/t ” oranları 10 ila 200 arasında değişmektedir. “ l/t ” oranları arttıkça yapıdaki tabakaların dağılımı artmaktadır. Bu polimerik nanokompozitin Young modülünde artışa neden olur. Organokil içeriği arttıkça, polimer nanokompozitin elastik modülü artar.

Grafiklerde çizgilerinin eğimlerinin, AYPE, DAYPE, PP (Buplen) Young modülleri farklarından dolayı, farklı olduğu gözlemlenmiştir. farklarından dolayı, farklı olduğu gözlemlenmiştir.

1. INTRODUCTION

Polymers have become very important in our daily lives. We make blends by mixing two homopolymers, composites by adding reinforcement fillers, nanocomposites by adding nano scale reinforcement particles. In order to form composite, polymer matrix and reinforcing element (usually two or more physically and chemically distinct phases) are joined and mechanical properties of the resulting product are better than individual components. The structure of the composite materials are mainly dependable on the component phase morphologies and interfacial properties. Nanoparticles show better mechanical properties than conventional reinforcement fillers when mixed around nanometer dimensional scale since interfacial area is higher than conventional composites. The reinforcing effect of nanoparticles is related to the l/t and the particle-matrix interactions. The nanoparticles are invisible to the naked eye because of its small size. Polyolefins (PO) are the most widely used polymers in preparation of polymer nanocomposites (PNC) and it is more difficult than that of any polymer, which contains polar groups in its backbone [1]. It is very hard to interact non-polar polymer and polar organoclay however, making PNC might be achieved with addition of a compatibilizer [2].

Homogeneous dispersion of nano-sized fillers in the matrix provides a large interfacial area more than conventional composites; otherwise the loosely agglomerated nanoparticles would easily result in failure of the composites when they are subjected to force. A homogeneous product, incorporation of any additives requires a serious mixing in molten state, which is primarily provided by melt blending process by means of extrusion.

In this study, different micromechanical models were studied and Halpin Tsai model was chosen to examine " l/t " of polyolefin nanocomposite as basis. Parameters are Young's modulus of pure matrix and final nanocomposite, mass and density of ingredients-nanoparticles. Mass and density is used to calculate filler volume fraction. Initially, this model was derived for fiber like reinforcement materials, however for platelet like fillers Modulus Reduction Factor (MRF) was included in

model for platelet type nanoparticles. The advantage of Halpin Tsai model is that it can be applied to many systems including different type of matrix material and filler types. Tactoid model (stack of nanoparticles) was developed for polyolefin nanocomposites for predicting properties. Since we can calculate aspect ratio of tactoids in nanocomposite structure from semi-empirical parameters, exfoliated or intercalated structure of PNC can be investigated from l/t values. Validity of modified Halpin Tsai model was examined with experiment results and theoretical values. Data used in calculations belongs to previously developed polyethylene and polypropylene nanocomposites and other universal values obtained from the literature.

2. THEORETICAL PART

Composite material consists of two or more components with different properties and distinct boundaries between the components. Majority of natural materials that have emerged as a result of a prolonged evolution process can be treated as composite materials. We can classify existing composite materials (composites) into two main groups.

The first group is known as “filled materials”. The main feature of this group is the existence of matrix material whose properties are improved by filling with particles. Matrix volume fraction is usually more than 50% in such materials, and matrix basically defines the properties of composite material. As a rule, filled materials can be treated as homogeneous and isotropic, i.e., traditional models of mechanics of materials developed for metals.

The second groups of composite materials are called “reinforced materials”. The basic components of these materials are long and thin fibers that provide the properties of high strength and stiffness, thus this group finds wide application in engineering. The fiber volume fraction in a composite is us usually less than 50% [3].

In polymer clay nanocomposites (PNC), clay minerals are randomly and homogeneously distributed in the polymer matrix in a few weight percentages. Mechanical, thermal and barrier properties of these materials are higher than virgin polymers and conventional composites on end-use product.

In 1985 PCN was invented at Toyota Central R&D Labs, Inc. (Toyota). This led to new applications for automotive, electric and food industries.

In conventional composites, polymers and stiffeners are not homogeneously mixed on a microscopic level, and are made up of different phases. The interface is not large, and interaction between the polymer (matrix) and the stiffener is limited. Takayanagi proposed the concept of a molecular composite, on the basis that if the filler is of molecular size then mechanical properties could be further improved, and

showed an example of a nylon matrix containing aramide fiber whose content was 5 weight % and diameter was 30 nm.

Toyota researchers considered that if platelets of nm dimensions were used instead of fibers, the contact surface would become much larger. Smectite clay minerals, especially montmorillonite (MMT), are potential candidates for a platelet-type filler for molecular composites, since they are composed of several layers of silicates. These silicates are 1 nm thick and have a cross-sectional area of 100 nm², which is very small compared to conventional stiffeners and also aramide fibers.

If the silicates are dispersed randomly and homogeneously in the polymer matrix, the interface area is enormous and a large interaction could be expected. If the silicates are in such a state, interactions between them must be avoided. Actually, it was discovered that when the clay content was less than 5 weight %, nanocomposite could be obtained. While some people classify PCN into the “intercalated” type, where the structure of the clay is maintained to some extent, and the “exfoliated” type, where silicate is randomly and homogeneously dispersed.

Each sample description refers to a specific composition involving the components used in the preparation of the samples.

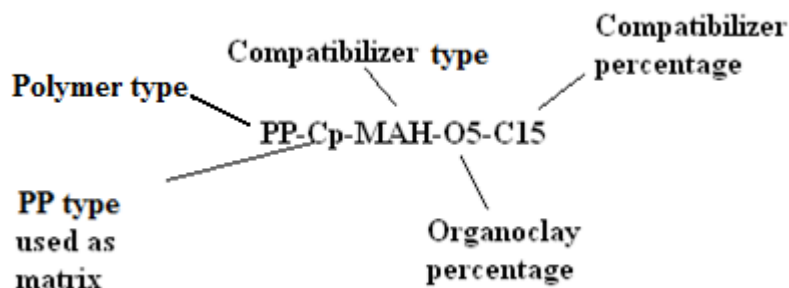


Figure 2.1 : Nomenclature of polymeric nanocomposites

In this work, theoretical elastic modulus of polypropylene nanocomposites was studied and compared with experimental results, from this approach “l/t” values were calculated, exfoliated intercalated structures are examined.

2.1 Clays

Smectite clays – mostly montmorillonite and hectorite have been mainly selected as fillers in polymer composites for industrial and scientific purpose since Toyota first invented the reinforcement in Nylon 6 by adding montmorillonite.

Chemists, materials scientists, physicists and geo-physicists have shown progress in applications about polymer-clay composites. Semi-empirical equations for relating the elastic modulus of particle-reinforced composites to the moduli of the components are generally enveloped by the Hashin and Shtrickman, Mori Tanaka, Halpin Tsai and Chris-Tensen models are most popular ones.

Natural montmorillonite in non-polar or low polarity polymers also makes conventional composites. Properties of nanocomposites can be experimentally controlled by reinforcement volume fraction ratio.

If polymer enters into clay galleries, the nanocomposite is ‘intercalated’. Generally amount of clay is less than 5%. As small amount of clay is used composite, a large amount of ‘free’ polymer forms the matrix and intercalated clay groups - tactoids - form the reinforcement. If the clay platelets are exfoliated in the polymer matrix, then the platelets provide the reinforcement. If clay stays in particle-form in the polymer matrix, the composite is ‘conventional’[5].

2. 1. 1 Structure and characteristics of layered silicates

Layered silicates, which are natural or synthetic minerals, are used in the synthesis of nanocomposites. They consist of very thin layers that are usually bound together with counter-ions. Basic building blocks of layered silicates are tetrahedral sheets in which silicon is surrounded by four oxygen atoms, and octahedral sheets in which a metal like aluminum is surrounded by eight oxygen atoms. In 1:1 layered structures (e.g. in kaolinite) a tetrahedral sheet is joined with an octahedral sheet, with shared oxygen atoms. Crystal lattice of 2:1 layered silicates consists of two-dimensional layers where a central octahedral sheet of alumina is fused to two external silica tetrahedra by the tip, so that the oxygen ions of the octahedral sheet also belong to the tetrahedral sheets, as shown in Fig. 2.1. The layer thickness is around 1 nm and

the lateral dimensions may differ from 300Å or higher. The layer thickness depends on the particulate silicate, the source of the clay and the method of preparation. Therefore length/thickness (l/t) ratio of these layers is high, in some circumstances these values are higher than 1000.

The basic 2:1 structure with silicon in the tetrahedral sheets and aluminum in the octahedral sheet contains no substitution of atoms. This structure is called pyrophyllite. As these layers do not expand in water, pyrophyllite has only an external surface area and no internal one. When silicon in the tetrahedral sheet is substituted by aluminum, the resulting structure is called mica. Substitution the mineral is characterized by a negative surface charge, which is balanced by interlayer potassium cations. Since size of the potassium ions matches the hexagonal hole created by the Si/Al tetrahedral layer, it is able to fit very tightly between the layers. Interlayers collapse and the layers are positioned by the electrostatic attraction between negatively charged tetrahedral layer and the potassium cations. As a result, micas do not swell in water. If in the original pyrophyllite structure the trivalent Al cation in the octahedral layer is partially substituted by the divalent Mg-cation, the structure of montmorillonite is formed. Montmorillonite is the best-known member of a group of smectite group clay minerals. In this case the overall negative charge is balanced by sodium and calcium ions. These sodium and calcium ions exist hydrated in the interlayer. These tetrahedral layers are held together by relatively weak forces since these ions do not fit in the tetrahedral layer as in mica. Water and other polar molecules can enter between the unit layers; this causes the lattice to expand.

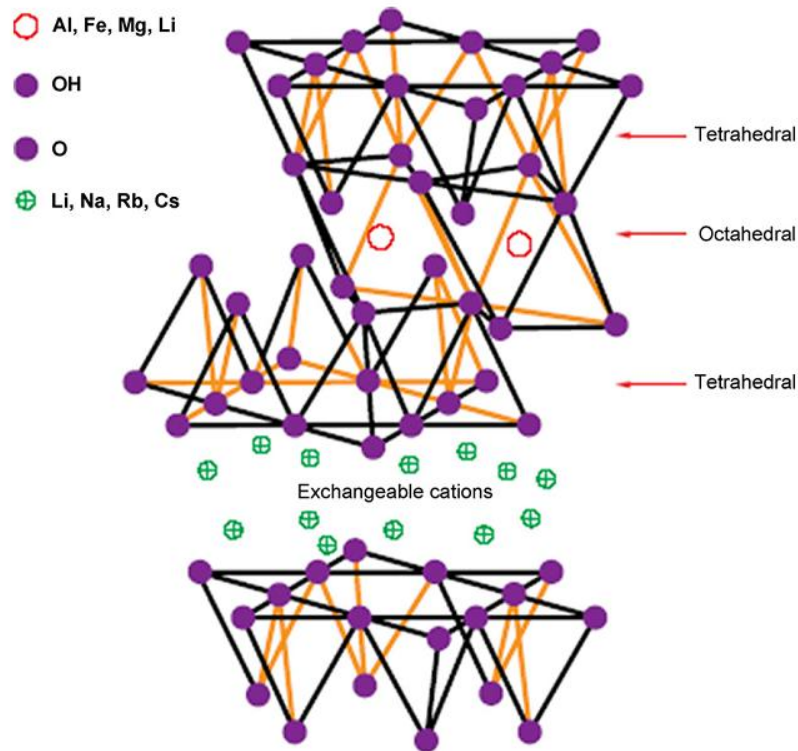


Figure 2.2 : Structure of a 2:1 layered silicate [6]

Hectorite and saponite are the layered silicates that are most commonly used in nanocomposite materials with montmorillonite. Chemical formulas of most commonly used layered silicates is given in Table 2.1.

Table 2.1: Chemical structure of commonly used 2:1 phyllosilicates [6].

2:1 Phyllosilicates	General Formula
Montmorillonite	$M_x(Al_{4-x}Mg_x)Si_8O_{20}(OH)_4$
Hectorite	$M_x(Mg_{6-x}Li_x)Si_8O_{20}(OH)_4$
Saponite	$M_xMg_6(Si_{8-x}Al_x)O_{20}(OH)_4$

High aspect ratio and unique intercalation/exfoliation characteristics took great attention as phyllosilicates are generally selected as reinforcing materials for polymers.

Generally, material perfection is nearly obtained as reinforcement element's dimensions become smaller. Reinforcement material's properties can be directly seen on composite on ultimate level if their dimensions reach atomic or molecular levels. For instance, carbon nanotubes exhibits highest known values of elastic modulus

(1.7 TPa) up to now. Individual 1 nm thick clay sheets also display a perfect crystalline structure. However, as reinforcing elements are smaller, their internal surface is larger, as a result they tend to form stacks rather than to disperse homogeneously in a matrix. The silicate layers have the tendency to organize themselves to form stacks with a regular van der Waals gap between them, called an “interlayer” or “gallery”. The interlayer dimension is determined by the crystal structure of the silicate. Dehydrated Na-montmorillonite’s interlayer dimension is approximately 1 nm.

There are levels of organization within the clay minerals. The smallest primary particles are on the order of 10 nm and are composed of stacks of parallel lamellae. Micro-aggregates are formed by combination of several primary particles, and aggregates are made up of several primary particles and micro-aggregates.

2.2 Polyethylene

Polyethylene (PE) is the highest-volume polymer in the world. It has high toughness, ductility, excellent chemical resistance, low water vapor permeability, and very low water absorption, easy processability. Low modulus, yield stress, and melting point limit the use of polyethylene. PE is used to make containers, bottles, film, and pipes. It is a versatile polymer with nearly limitless variety due to copolymerization potential and wide density range. Molecular weight (MW) ranges from very low (waxes have an MW of a few hundred) to very high (6×10^6).

Ethylene has various polymerization mechanisms. Its repeat structure is $(-\text{CH}_2\text{CH}_2-)_x$, which is written as polyethylene rather than polymethylene $(-\text{CH}_2)_x$. PE homopolymers are made up of carbon and hydrogen atoms, just as the properties of diamond and graphite deceptively. Different grades of PE have different thermal and mechanical properties. Polyethylene is generally whitish, semi-opaque, and available in grades of density that range from 0.91 to 0.97 g/cm³. Morphology of the backbone affects the density of a particular grade. Long, linear chains with very few side branches can assume a much more three-dimensionally compact, regular, crystalline structure. Generally, yield strength and the melt temperature increase with density, while elongation decreases with increased density.

Four established production methods of polyethylene are 1- a gas phase method known as the Unipol process, practiced by Union Carbide, 2- a solution method used by Dow and DuPont, 3- a slurry emulsion method practiced by Phillips, and 4- a high-pressure method [6].

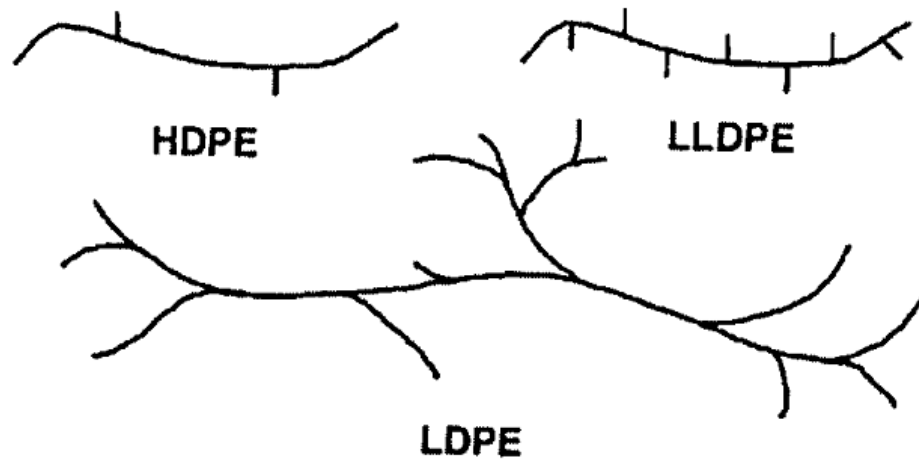


Figure 2.3 : Chain configurations of polyethylene [6]

2.2.1.1 Low Density Polyethylene (LDPE)

LDPE is mainly used in packaging films because of its high impact strength, toughness, and ductility. Films range from shrink film, thin film for automatic packaging, heavy sacking, and multilayer films (both laminated and coextruded) where LDPE acts as a seal layer or a water vapor barrier. LLDPE has higher melt strength than LDPE in film applications. However, LDPE is still very widely used, and formed via free radical polymerization, with alkyl branch groups given by the structure $-(CH_2)_xCH_3]$ of two to eight carbon atom lengths. The most common branch length is four carbons long. High reaction pressures increase the amount of crystalline regions. The reaction to form LDPE is shown in Fig. 2.3, where “n” approximately varies in commercial grades between 400 and 50,000.

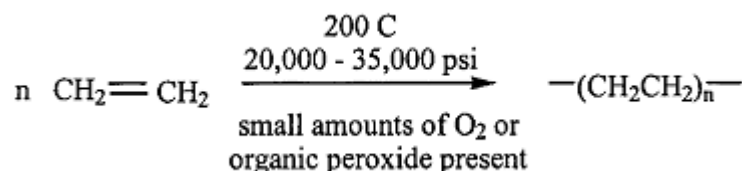


Figure 2.4 : Polymerization of PE [6]

2.2.1.2 Linear Low Density Polyethylene (LLDPE)

LLDPE has enhanced tensile strength for the same density of LDPE. Table 2.2 compares mechanical properties of LLDPE to LDPE. LLDPE is a long linear chain without long side chains or branches. The short chains prevent crystalline formation and formation of high density PE's are obstructed. Lower polymerization pressures and temperatures are required for LLDPE compared with LDPE with latest developments. A typical LDPE process requires 35,000 lb/in², which is reduced to 300 lb/in² in the case of LLDPE, and reaction temperatures as low as 100°C rather than 200 to 300°C are used. LLDPE is actually a copolymer containing most commonly side branches of 1-butene, also with 1-hexene or 1-octene. Density ranges of 0.915 to 0.940 g/cm³ polyethylenes are polymerized with Ziegler catalysts. These catalysts orient the polymer chain and govern the tacticity of the pendant side groups [6].

Table 2.2: Comparison of Blown Film Properties of LLDPE and LDPE [6]

Property	LLDPE	LDPE
Density g/cm ³	0.918	0.918
Melt index, g/10 min	2.0	2.0
Dart impact, g	110	110
Puncture energy, J/mm	60	25
Machine-direction tensile strength, MPa	33	20
Cross-direction tensile strength, %	25	18
Machine-direction tensile elongation, %	690	300
Cross-direction tensile elongation, %	740	500
Machine-direction modulus, MPa	210	145
Cross-direction modulus, MPa	350	175

2.2.1.3 Metallocene Catalysed Polyethylene

Metallocene catalysed polyethylenes are like low density polyethylenes (LDPE and LLDPE) than HDPE. As with LLDPE they are usually copolymers containing small quantities of a low molecular weight α -olefin such as but-1-ene, hex-1-ene and oct-1-ene. The property differences of m-PE largely come out from the narrow molecular weight distribution, the more uniform incorporation of the α -olefin and the

low level of polymerization residues.

It is generally claimed that metallocene polyethylenes (often abbreviated to m-PE) exhibit superior mechanical and optical properties. m-LLDPE is favored as a stretch film for wrapping because of the better prestretchability, higher puncture resistance and tear strength than conventional LLDPE.

Narrow molecular weight distribution polymers such as m-PE are less pseudoplastic in their melt flow behaviour than conventional polyethylenes. m-LLDPE and a conventional LLDPE of have similar melt index at low shear rates. The m-LLDPE will have a much higher melt viscosity at the high shear rates than LLDPE; usually involved in film processing. The polymers are also more susceptible to melt fracture and sharkskin. This difference requires using more highly powered extruders, using special processing aids such as fluoroelastomers or making agreement in the polymer structure which reduce the advantages of m-PE materials. One approach would be to produce bi-, tri- or other polymodal blends to overcome disadvantages of narrow molecular weight distribution polymers.

Metallocene - catalyzed very low density polyethylene (m-VLDPE) has become available with densities of as low as 0.903. This useful for sealing layers of multilayer films since sealing can commence at lower temperatures than with conventional materials such as LLDPE and EVA.

2.2.2 Structure and Properties of Polyethylene

The polyethylene is long chain aliphatic hydrocarbon of the type and thermoplastic.

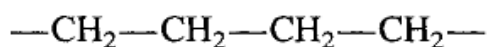


Figure 2.5 : Polyethylene structure [6]

The flexibility of the C-C bonds would be expected to lead to low values for the glass transition temperature. The T_g is associated with the motion of comparatively long segments in amorphous matter. Since in a crystalline polymer there are only a small number of such segments, the T_g has little physical significance. In fact there is considerable argument as to the position of the T_g and amongst the values quoted in the literature are -130°C , -120°C , -105°C , -93°C , -81°C , -77°C , -63°C , 48°C , -30°C , -20°C and $+60^\circ\text{C}$. Some data on the crystalline structure of polyethylene are

summarized in Table 2.3. There are no strong intermolecular forces. The high crystallinity also leads to opaque structures except in the case of rapidly chilled film where the development of large crystalline structures is prevented.

Polyethylene is expected to have a good resistance to chemical attack and this is found to be the case.

Polyethylene has a low cohesive energy density. Because it is a crystalline material and does not enter into specific interaction with any liquids, there is no solvent at room temperature. At elevated temperatures the thermodynamics are more favorable to solution and the polymer dissolves in a number of hydrocarbons of similar solubility parameter.

Table 2.3: Crystallinity data for Polyethylene [6]

Property	Value
Molecular disposition	planar zigzag
Unit cell dimensions	a = 7.36 Å b = 4.92 Å c = 2.54 Å
Cell density (unbrached polymer) (25 °C)	1.014
Amorphous density (20 °C)	0.84

The polyethylene is expected to be an excellent high-frequency insulator because of its non-polar nature.

At the present time there are available many hundreds of grades of polyethylene, most of which differ in their properties in one way or another. Such differences arise from the following variables:

- (1) Variation in the degree of short chain branching in the polymer.
- (2) Variation in the degree of long chain branching.
- (3) Variation in the average molecular weight.
- (4) Variation in the molecular weight distribution (which may in part depend on
- (5) The presence of a small amount of co monomer residues.
- (6) The presence of impurities or polymerization residues.

Further variations can also be obtained by compounding and cross-linking the polymer.

The more recently developed linear low-density polyethylenes are free of long chain branches but do contain short side chains as a result of copolymerizing ethylene with a smaller amount of a higher alkene such as oct-1-ene. Such branching interferes with

the ability of the polymer to crystallize, as with the older low-density polymers and like them have low densities. The word linear in this case is used to imply the absence of long chain branches.

Differences in molecular weight will also give rise to differences in properties. The higher the molecular weight, the greater the number of points of attraction and entanglement between molecules. Differences in short chain branching and (hence degree of crystallinity) largely affect properties characterized by small solid displacement. Molecular weight differences will affect properties that involve large deformations such as ultimate tensile strength, elongation at break, melt viscosity and low-temperature brittle point. There is also an improvement in resistance to environmental stress cracking with increase in molecular weight.

Commercial polyethylenes vary in their molecular weight distribution (MWD). Whilst for some purposes a full description of the distribution is required, the ratio of weight average molecular weight to number average molecular weight provides a useful parameter. Its main deficiency is that it provides no information about any unusual high or low molecular weight tail which might have profound significance.

Much of recent development in polymerization technology has been devoted to establishing control of the MWD of LLDPE polymers. With such polymers, narrowing the MWD confers higher toughness, greater clarity, lower heat seal initiation temperatures and, where this is important, higher cross-link efficiency. As with LDPE there is lower melt shear sensitivity and poorer melt strength.

2.2.3 Mechanical Properties of Polyethylene

The mechanical properties are very dependent on the molecular weight and on the degree of branching of the polymer. As with other polymers these properties are also dependent on the rate of testing, the temperature of test, the method of specimen preparation, the size and shape of the specimen and, to only a small degree with polyethylene, the conditioning of samples before testing. The figures given show clearly the general effects of branching (density) and molecular weight on some polymer properties. Under different test conditions, different results may be obtained. Also polymers of different density but with the same melt flow index do not have the same molecular weight. The general effects of changing rate of testing, temperature and density on the tensile stress-strain curves are shown in Figure 2.5.

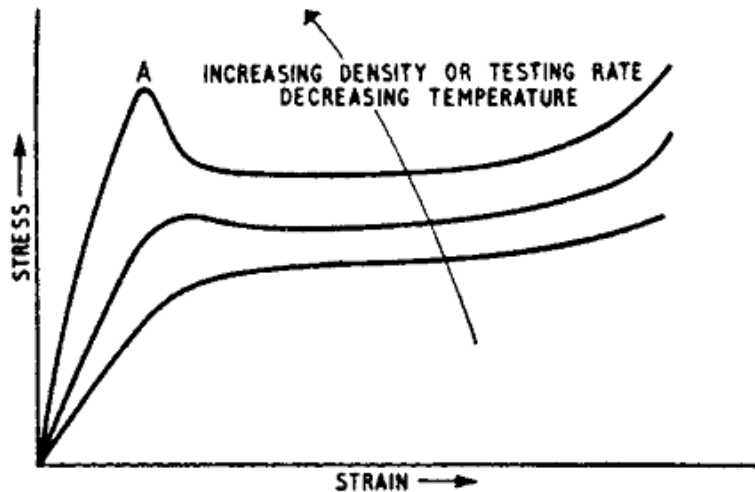


Figure 2.6 : Effect of polymer density, testing rage and temperature on the shape of the stress-strain curve for polyethylene [7]

It is seen in particular that as the test temperature is lowered or the testing rate increased, a pronounced ‘hump’ in the curve becomes apparent, the apex of the hump A being the yield point. Up to the yield point deformations are recoverable and the polymer is almost Hookean in its behavior. The working of the sample, causes ‘strain softening’. This cold drawing causes molecular orientation and induces crystallization so that there is a stiffening of the sample and an upward sweep of the stress-strain curve.

The effect of temperature on a sample of low density polyethylene with an MFI of 2 is shown in Figure 2.6.

The varying influence of rate of strain on tests results can be shown from figures obtained with two commercial polyethylene samples (Table 2.4). It is seen that in one case an increase in rate of strain is accompanied by increase in tensile strength and in the other case, reduction.

Table 2.4: Effect of straining rate on the measured tensile strength and elongation at break of two samples of polyethylene [7]

Rate of strain (in/min)	Tensile strength (MPa)	
	Polymer A	Polymer B
6	18.48	11.03
12	18.96	10.90
18	20.00	10.34
30	22.07	9.66
	Elongation at break (%)	
6	380	450
12	300	490
18	200	490
30	180	500

The elongation at break of polyethylene is strongly dependent on density, the more highly crystalline high-density materials being less ductile. This lack of ductility results in high-density polymers tending to be brittle, particularly with low molecular weight materials.

Under load polyethylene will deform continuously with time ('creep'). A knowledge of creep behavior is important when considering load-bearing applications, water piping being a case in point with polyethylene. In general, there will be an increase in creep with increased load, increased temperature and decreased density. A large amount of creep data has been made available in specialized monographs and in trade literature [7].

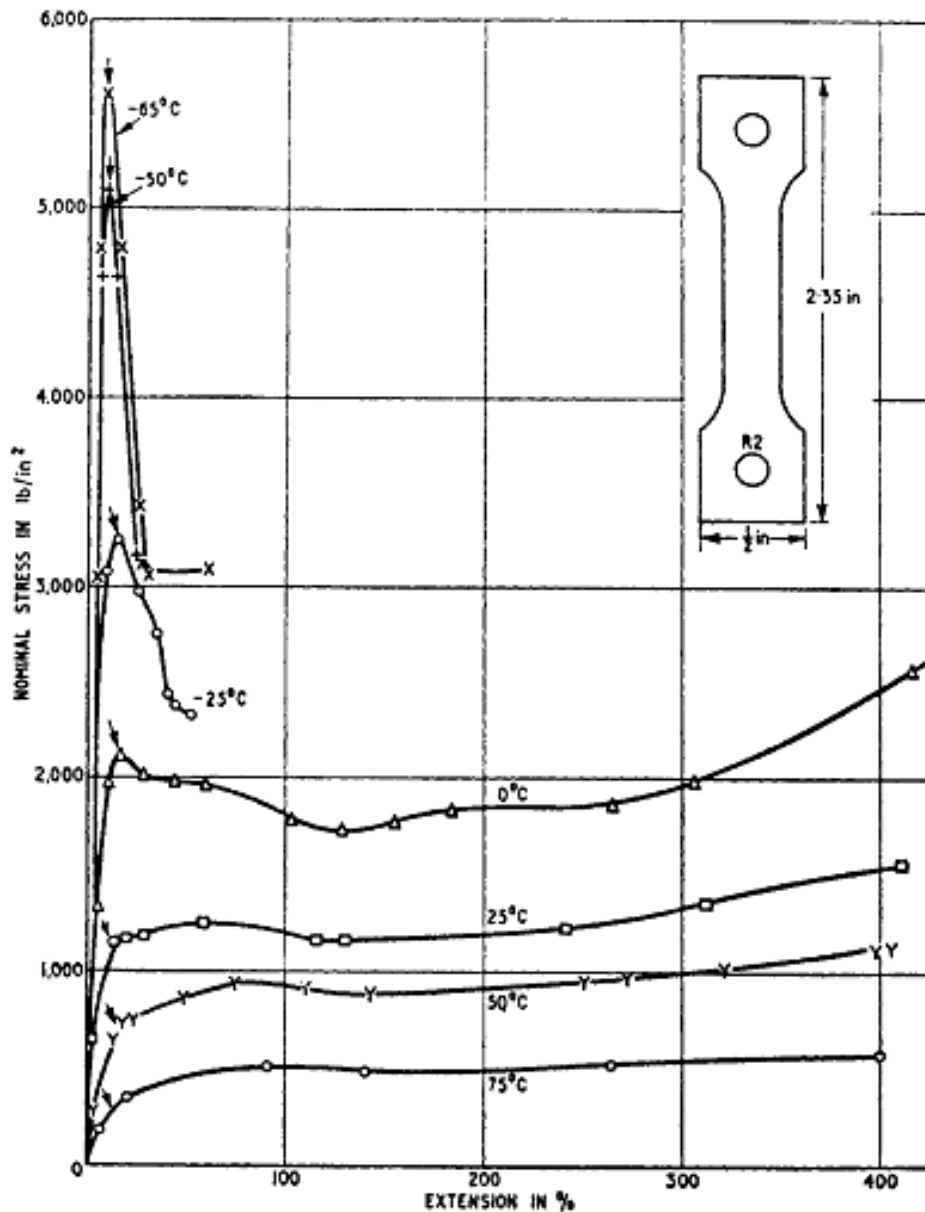


Figure 2.7 : Effect of temperature on the tensile stress-strain for polyethylene.
 (Low-density polymer $\sim 0.92 \text{ g/cm}^3$, MFI=2.) Rate of extension
 190% per minute [7]

2. 3 Polypropylene

Polypropylene is a multipurpose polymer used in applications from films to fibers and automotive & electronic parts. Polypropylene's worldwide demand is 9.5 million kilograms. It is similar to polyethylene in structure, except for the substitution of one hydrogen with a methyl group on every other carbon. As a result, different stereo isomers are formed. Syndiotactic, isotactic, and atactic configurations are shown in Fig. 2.8.

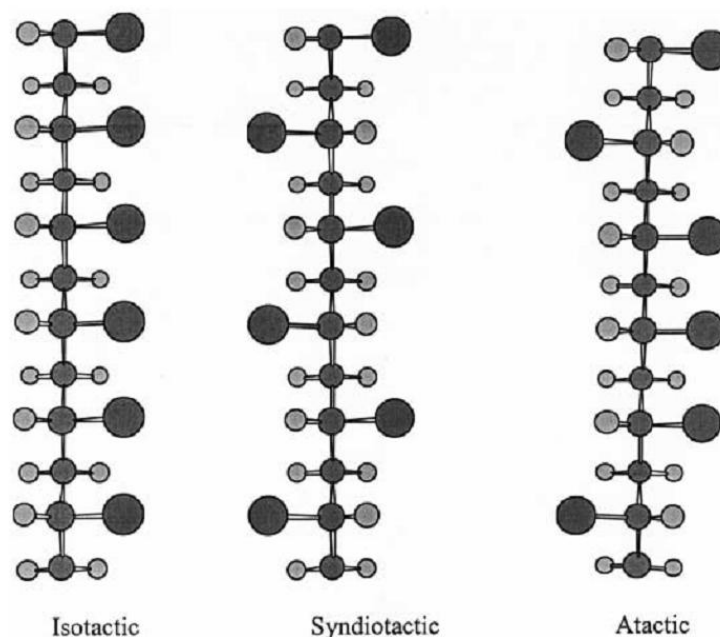


Figure 2.8 : Isotactic, syndiotactic, and atactic polymer chains.[7]

Polypropylene (PP) is synthesized by the polymerization of propylene as shown in Fig. 2.9; Propylene is a monomer derived from petroleum products. Polypropylene could be polymerized commercially after usage of Ziegler-Natta catalysts. These catalysts allowed the control of stereochemistry during polymerization to form polypropylene in the isotactic and syndiotactic forms, more crystalline form than a tactic state. The first commercial method for the production of polypropylene was a suspension process. Current production methods include gas phase and liquid slurry processes. Metallocene catalysts are used in polymerization of new grades of polypropylene. The range of molecular weights for PP is $M_n = 38,000$ to $60,000$ and $M_w = 220,000$ to $700,000$. Polydispersity index (M_n/M_w) is between 2 and 11.

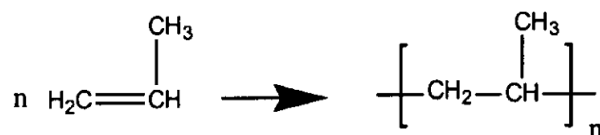


Fig. 2.9 : Polymerization of Polypropylene [8]

Three stereo isomers show different behaviors. Isotactic and syndiotactic polypropylene can pack into a regular crystalline array. Crystal region makes these types more rigid. Syndiotactic polypropylene has lower T_m than the isotactic polymer. The isotactic polymer is the most commercially used form with a melting point of 165°C . Atactic polypropylene has a very small amount of crystallinity about

5 to 10 percent. Since its irregular structure prevents crystallization; atactic polypropylene behaves like soft flexible material. It is used in applications such as sealing strips, paper laminating, and adhesives.

Commercial polymers are about 90 to 95 percent isotactic. The amount of isotacticity in the chain will influence the properties. As the amount of isotactic material increases, the amount of crystallinity will also increase. This results an increase in elastic modulus, softening point, and hardness.

Polypropylene is similar to polyethylene in many points, for example, they are both saturated hydrocarbon polymers, but they differ in some significant properties. Isotactic polypropylene is harder and has higher softening point than polyethylene, so it is used where stiff components are used. Polypropylene has better environmental stress cracking resistance than polypropylene but less resistant to degradation - particularly high temperature oxidation. Tertiary carbons in PP decrease degradation resistance. This allows easier hydrogen abstraction compared with PE. As a result, antioxidants are added to polypropylene to improve the oxidation resistance. Polyethylene and polypropylene's degradation mechanisms are different. PE crosslinks on oxidation and PP chains break. High-energy radiation is also a method for cross linking polyethylene.

Polypropylene has a density of 0.905 g/cm^3 , makes it one of the lightest plastics. Polypropylene has low water absorption because it has nonpolar nature. Polypropylene has good chemical resistance, but liquids such as chlorinated solvents, gasoline, and xylene can affect the material. Polypropylene has a low dielectric constant and is a good insulator. Adhesion characteristics can be improved by usage of surface treatments.

Polypropylene has a higher T_g and melting point than polyethylene except ultra high molecular weight polyethylene. Polypropylene needs to be processed at higher temperatures than polyethylene. PP can withstand boiling water and can be used in applications requiring steam sterilization because of higher softening point. Polypropylene is also more resistant to cracking in bending than PE and is preferred in applications that require tolerance to bending. Applications that require long-term dynamic flexibility such as ropes, tapes, carpet fibers, is available by polypropylene. Polypropylene is brittle at low temperatures about 0°C . This can be improved through copolymerization with other polymers such as ethylene.

Polypropylene can be processed by similar methods with PE. Melting temperature of different kinds of polypropylene is between the range of 210 and 250°C. Heating period should be minimized to reduce the possibility of oxidation. Blow molding of PP is more difficult than PE because PP requires the use of higher melt temperatures and shear; process conditions accelerate the degradation of PP. The screw-metering zone should not be too superficial to avoid excessive shear.

In film applications, transparency requires careful control of the crystal growth. This can be achieved in blown film by extruding downward into two converging boards. In the Shell process, the boards are covered with a film of flowing, cooling water. Oriented films of PP are manufactured by passing the PP film into a heated area and stretching the film both transversely and longitudinally. Film may be annealed at 100°C to reduce shrinkage while under tension. Highly oriented films may show low strength in width and a tendency to make irregular, rapid movements. Other polypropylene manufacturing methods include sheet (for thermoforming) and profile extrusion.

Short glass reinforcement can be added for increasing stiffness. Coupling agents can improve the properties of glass-filled PP. Stiffness of polypropylene can also be improved by calcium carbonate and talc.

Other additives, such as pigments, antioxidants, and nucleating agents, can be blended into polypropylene to give the desired properties. Carbon black is often added to polypropylene to provide UV resistance in outdoor applications. Anti blocking and slip agents may be added for film applications to decrease friction and prevent sticking. Antistatic agents can be added for packaging applications.

Addition of rubber to polypropylene can result improvements in impact resistance. One of the most commonly added elastomers is ethylene-propylene rubber. When elastomer is blended with polypropylene, separate elastomer phase is formed. Elastomeric compositions can be done in excess addition of 50 percent. If less than 50 percent rubber is added to PP, it can be called modified thermoplastic. Impact grades of PP can be formed into films with good penetration resistance.

Copolymers of polypropylene with other monomers such as ethylene are also available. Copolymers usually contain between 1 to 7 weight percent of ethylene randomly placed in the polypropylene backbone. This hinders the tendency of the polymer chain to crystallize, results more flexible products. Copolymerization increases flexibility, decreases melting point, improves impact resistance. Increase in

ethylene content increases flexibility, eventually turning the polymer into an elastomer (ethylene propylene rubber). Polypropylene copolymers also exhibit increased clarity and are used in blow molding, injection molding, and extrusion.

Polypropylene films are used in a variety of packaging applications. Both oriented and non-oriented films are used. Film tapes are used for carpet backing and sacks. Foamed sheet is used in a variety of applications including thermoformed packaging. Fibers are another important application for polypropylene, particularly in carpeting, because of its low cost and wear resistance. Fibers prepared from polypropylene are used in both woven and nonwoven fabrics [8].

2. 3. 1 Structure and properties of Polypropylene

Polypropylene and polyethylene have many similarities in their properties, particularly in their swelling and solution behavior and in their electrical properties. Methyl group attached to alternate carbon atoms on the chain backbone can alter the properties of the polymer in a number of ways. Isotacticity and syndiotacticity can cause a slight stiffening of the chain, increase in the crystalline melting point. In the most regular circumstances, polypropylene's melting point is 50°C higher than polyethylene. The methyl side groups can also influence some points of chemical behavior. For example, the tertiary carbon atom provides a site for oxidation so that the polymer would be less stable than polyethylene to the influence of oxygen. In addition, thermal and high energy treatment leads to chain split rather than crosslinking.

In three forms of tacticity, isotactic form cannot crystallize in a planar zigzag form because of the steric hindrance of the methyl groups but crystallize in a helix, with three molecules being required for one turn of the helix. Both right-hand and left-hand helices occur but both forms can fit into the same crystal structure. Commercial polymers are usually about 90-95% isotactic. Atactic and syndiotactic structures may be present as either complete molecules or blocks of varying length in chains of isotactic molecules in commercial polymers. Stereo block polymers may also be formed in which a block of monomer remains with a right-handed helix is succeeded by a block with a left-handed helix. The frequency with which such changes in the helix direction occur can have an important influence on the crystallization and bulk properties of the polymer. It's difficult to give full description of a specific propylene polymer in practice although there has been

marked progress in recent years. Many manufacturers simply state that their products are highly isotactic, others quote the polymer crystallinity obtained after some specified annealing treatment, whilst others quote the so-called 'isotactic index'. Isotactic index is the percentage of polymer insoluble in n-heptane. Both of these last two properties provide rough measure of the isotacticity but these measures do not have high precision. For example the isotactic index is affected by two parameters, first one is high molecular weight atactic polymer which is insoluble in n-heptane and second one is the presence of block copolymers of isotactic and atactic structures.

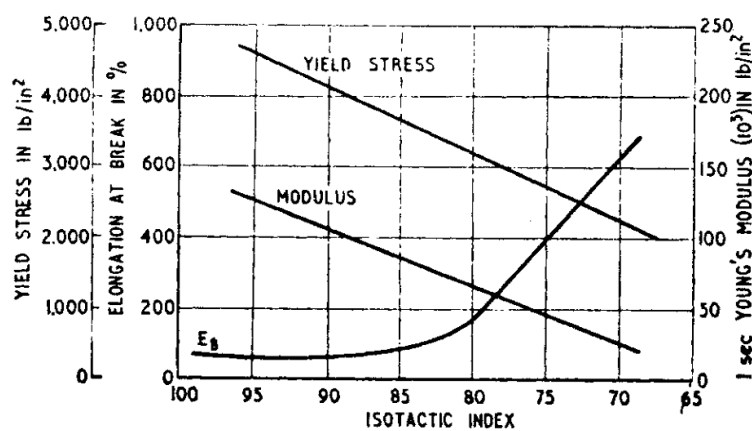


Figure 2.10 : Effect of isotacticity on tensile properties [9]

General effects of different the degree of isotacticity are well known, in spite of these problems. Atactic polymer is an amorphous and little bit rubbery, on the other hand the isotactic polymer is stiff, highly crystalline and has high melting point. Within the range of commercial polymers, the greater the amount of isotactic material the greater the crystallinity and the greater the softening point, stiffness, tensile strength, modulus and hardness. All other structural features are equal. (Figure 2.9).

The influence of molecular weight on the bulk properties of polypropylene is often opposite to that experienced with most other well known polymers. Although an increase in molecular weight leads to an increase in melt viscosity and impact strength, it also leads to a lower yield strength, lower hardness, lower stiffness and softening point in accord with most other polymers. Reason of this effect is believed that high molecular weight polymer does not crystallize so easily as lower molecular weight material and differences in the degree of crystallization affect the bulk properties. It may also be stated that an increase in molecular weight causes reduction in brittle point (see Table 2.5).

Table 2.5: Some mechanical and thermal properties of commercial polypropylenes [9]

Property	Test Method	Homopolymers			Copolymers	
Melt flow index	(a)	3.0	0.7	0.2	3.0	0.2
Tensile strength (lbf/in ²)		5000	4400	4200	4200	3700
(MPa)	(b)	34	30	29	29	25
Elongation at break (%)	(b)	350	115	175	40	240
Flexural modulus (lbf/in ²)		190000	170000	160000	187000	150000
(MPa)	-	1310	1170	1100	1290	1030
Brittleness temperature (°C)	ICI/AST M					
	D.476	+15	0	0	-15	-20
Vicat softening point (°C)	BS 2782	145-150	148	148	148	147
Rockwell hardness(R-scale)	-	95	90	90	95	88.5
Impact Strength (ft lbf)	(c)	10	25	34	34	42.5
(J)	13.5	34	46	46	57.5	

(a) Standard polyethylene grader: load 2.16kg at 230°C.

(b) Straining rate 18 in/min.

(c) Falling weight test on 14 in diameter moulded bowls at 20°C

As shown in table the mechanical and thermal properties of polypropylene are dependent on the molecular weight and on other structure features. The properties of five commercial materials (all made by the same manufacturer and subjected to the same test methods) which are of approximately the same isotactic content but which differ in molecular weight and in being either homopolymers or block copolymers are compared in Table 2.5.

The figures in Table 2.5 show quite clearly how an increase in molecular weight (decrease in melt flow index) causes a reduction in tensile strength, stiffness, hardness and brittle point but an increase in impact strength.

Limited amount of information is available about effects of molecular weight distribution. However, there is evidence that the narrower the distribution, the more newtonian are the melt flow properties. It has been observed that with polymers of

molecular weights suitable for molding and extrusion, polymers that has wide distribution are stiffer and more brittle.

The morphological structure of polypropylene is rather complex and at least four different types of spherulites have been observed. The properties of the polymer will depend on the size and type of crystal structure formed and this will turn to be dependent on the relative rates of nucleation to crystal growth. The ratio of these two rates can be controlled by differentiating the rate of cooling and the incorporation of nucleating agents. In general, the smaller the crystal structures, the greater the transparency and flex resistance, the less the rigidity and heat resistance.

Polypropylene has dominating transition point which occurs at about 0°C at about which polymer becomes brittle. Even at room temperature the impact strength of some grades leaves something to be desired. Products of improved strength and lower brittle points may be obtained by block copolymerization of propylene with small amounts of ethylene. Such propylene copolymers are widely used and are often preferred to the homopolymer in injection molding and bottle blowing applications [9].

2.3.2 Mechanical properties of Polypropylene

Stiffness, strength, and impact resistance are most important mechanical properties in plastic product design. Stiffness is measured as the flexural modulus, determined in a flexural test, and impact resistance by a number of different impact tests, with the historical favorite being the izod impact at ambient and at subambient temperatures. These mechanical properties are generally used to predict the properties of molded articles. Strength is usually defined by the stress at the yield point rather than by the strength at break, but breaking strength is usually specified for fiber or film materials under tensile stress.

Mechanical properties of polymers are measured on specimens fabricated from resins, so processing conditions and testing procedures effect the use and comparison of mechanical property data. Because there are so many variables that can affect mechanical properties, consensus testing organizations like ASTM and ISO were formed to bring some uniformity and consistency to specimen preparation and mechanical testing. Because the ASTM and ISO fabrication and testing methods allow some freedom within their guidelines, when one is asked what the mechanical properties of a material are, the first answer should be to ask by what tests, what

specimens, and under what conditions. The latter includes such factors as the exact specimen type, age of specimen, how the specimen was conditioned, testing speed, testing temperature, data acquisition procedure, and method of calculation.

Flexural modulus or stiffness increases as the level of crystallinity increases in a PP product, crystal morphology also effects modulus. Thus, stiffness generally decreases as the crystallizability (tacticity) decreases or, in random copolymers, crystallizability decreases directly proportional to amount of ethylene content [10].

Fillers, reinforcement and modifiers change mechanical properties of Polypropylene. If the fibers are not chemically coupled to polymer matrix, tensile strength is not greatly affected by fillers, nor even by glass fiber reinforcement. If the coupling efficiency increases, there is improvement on the tensile load transferred from the PP matrix to the reinforcing fibers. Flexural modulus, or rigidity, is improved by fillers such as talc and calcium carbonate, as well as by reinforcements. Impact strength is reduced by fillers but increased by elastomers modifiers. Impact strength increases as the temperature rises and material becomes more elastic and ductile [11].

2.4 Melt Flow Index

Melt Flow Index is the output rate (flow) in grams that occurs in 10 minutes through a standard die of 2.0955 ± 0.0051 mm diameter and 8.000 ± 0.025 mm in length when a fixed pressure is applied to the melt via a piston and a load of total mass of 2.16 kg at a temperature of 190°C (some polymers are measured at a higher temperature, some use different weights and some even different orifice sizes).

Melt Flow Index is an assessment of average molecular mass and is an inverse measure of the melt viscosity; in other words, the higher a MFI, the more polymer flows under test conditions. Knowing the MFI of a polymer is vital to anticipating and controlling its processing. Generally, higher MFI polymers are used in injection moldings, and lower MFI polymers are used with blow molding or extrusion processes.

Many factors affect polymer's flow properties. Molecular weight distribution, the presence of co-monomers, the degree of chain branching and crystallinity influence a polymer's MFI as well as heat transfer in polymer processing.

2.5 Compatibilizers

Compatibilizers are interfacial agents that improve compatibility between immiscible polymer blends and composites with the effect of wetting, dispersion and adhesion. Compatibilizer term is commonly used for immiscible polymer blends; for dispersed fillers “coupling agents” or “surface modifiers” are commonly used. They are all considered as interfacial agent. There are differences and similarities in the compatibilization mechanisms applicable to blends and composites.

Incompatibility of polymers is major difficulty in devising a useful polymer blend. There is no entropy of mixing for a blend of high molecular weight polymers. Thus, one major driving force for solubility that is found in mixtures of small is absent in polymer blends. Therefore, it is possible to expect that polymers will be soluble or miscible in one another only in special cases, such as in the presence of specific strong interactions between repeating units. This issue has been explained in different texts. Rarer still is immiscibility and compatibility at which a mixture's constituents have different properties such as structure, polarity but show some interaction, because of reactive groups, surface active agents, or compatibilizers [12]. Technology of toughened polymers is based on immiscibility and compatibility, it synergistically combines the properties of completely different polymers to form a blend with properties superior to those of the individual blend components [13].

LDPE-g-MMI, LLDPE-g-MMI, LDPE-g-IA, LLDPE-g-MMI, mLLDPE-g-IA, PP-g-IA were used as compatibilizers in this work.

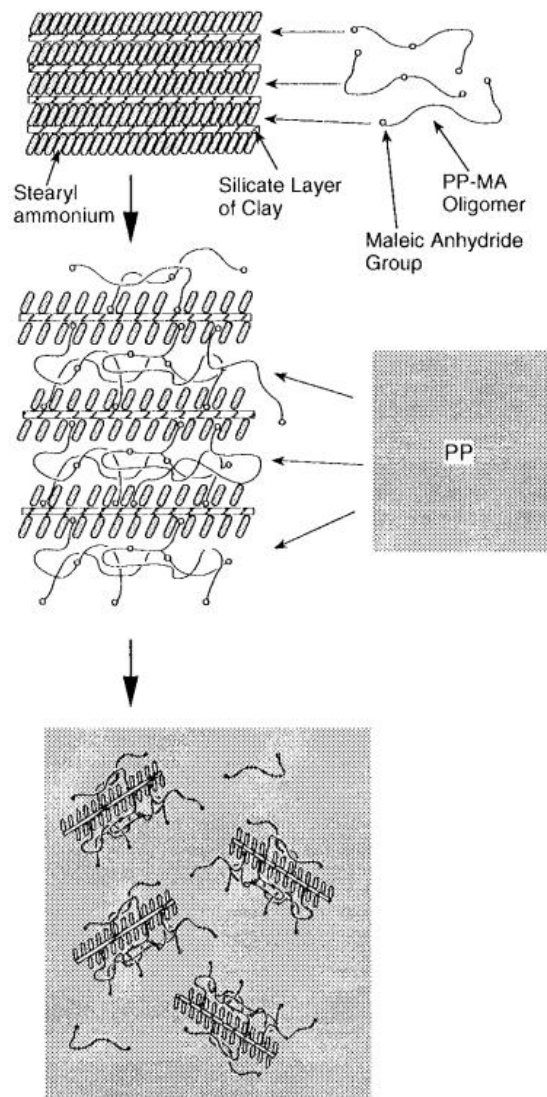


Figure 2.11 : Schematic representation of the dispersion process of the organized clay in the PP matrix with the aid of PP-g-MAH [14]

2.6 Polymer Nanocomposites

A composite material is made by combining two or more materials to give a unique combination of properties. Nanocomposite technology is a newly developed field, in which nanofillers are added to a polymer to reinforce and provide novel characteristics. Nanocomposite technology is applicable to a wide range of polymers from thermoplastics and thermosets to elastomers.

2.6.1 Polymer nanocomposite preparation and synthesis

The process of synthesis of polymer/clay nanocomposites involves the uniform dispersion of agglomerates of clay particles within a polymeric matrix. Ultimately, the nanocomposites would incorporate smaller intercalated clay particles, fully

exfoliated individual clay platelets, or a mixed intercalated/exfoliated system. In order to qualify as a nanocomposite, this exhibits useful mechanical, barrier, electrical, thermal, and other properties [15].

Colloid and surface chemistry play important roles in the synthesis of polymer-clay nanocomposites. Dispersion of clay layers in polymers is hindered by the inherent tendency to form face-to-face stacks in agglomerated tactoids due to high interlayer cohesive energy. There is a growing interest in the surface chemistry of clays in pursuit of nanocomposite synthesis using specific monomers, prepolymers and polymer melts. Polymers and silicates do not necessarily form a nanocomposite: the compatibility between the two phases is important [16].

In general, nanocomposites can be formed in one of three ways:

- Melt intercalation.
- Solution dispersion.
- In-situ polymerization.

2.6.1.1 Melt intercalation

Melt intercalation is the most widely used method in polymer/clay nanocomposite preparation, and it has tremendous potential for industrial application. An advantage of this method over the others is that no solvent is required. The melt blending process involves mixing the layered silicate by annealing, statically or under shear, with polymer pellets while heating the mixture above the softening point of the polymer. During the annealing process, the polymer chains diffuse from bulk polymer melt into the galleries between silicate layers.

Figure 2.11 represents a schematic illustration of nanocomposite formation by direct melt intercalation structure and properties of organically modified layered silicate. This process involves annealing a mixture of the polymer and organically modified layered silicate above the softening point of the polymer, statically or under shear. While annealing, the polymer chains diffuse from the bulk polymer melt into the galleries between the silicate layers [15][17].

In some cases the polymer–silicate mixture can be extruded by using (a) static melt intercalation: by mixing and grinding dried powders of polymer and organic silicate in a pestle and mortar and then heating the mixture in vacuum, and (b) extrusion melt intercalation: by extruding the mixture with twin screw extruder to produce a polymer nanocomposite from the polymer and modified clay [18] [19].

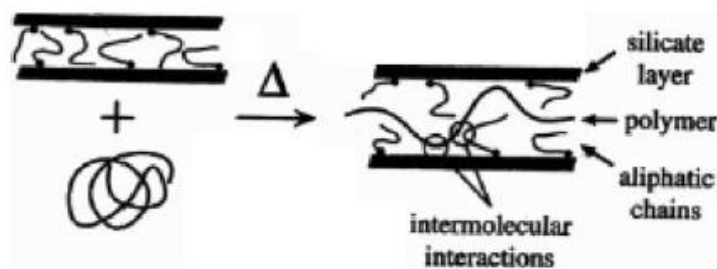


Figure 2.12 : Schematic depicting the intercalation process between a polymer melt and an organically modified layered silicate [15]

2.6.1.2 Solution dispersion

The solution dispersion method involves mixing a preformed polymer solution with clay. This is based on a solvent system in which the polymer or pre-polymer is soluble and the silicate layers are swellable. The layered silicate is first swollen in a solvent, such as water, chloroform, or toluene. When the polymer and layered silicate solutions are mixed, the polymer chains intercalate and displace the solvent within the interlayer of the silicate. Upon solvent removal, the intercalated structure remains, resulting in polymer / layered silicate nanocomposite. Using this method, intercalation only occurs for certain polymer/solvent pairs. This method is good for the intercalation of polymers with little or no polarity into layered structures, and facilitates production of thin films with polymer-oriented clay intercalated layers. However, from commercial point of view, this method involves the copious use of organic solvent, which is usually environmentally unfriendly and economically prohibitive [15] [20].

2.6.1.3 In-situ polymerization

In-situ polymerization involves the dispersion and distribution of clay layers in the monomer followed by polymerization (Figure 2.12). The layered silicate is swollen within the liquid monomer or a monomer solution so that polymer formation can occur between the intercalated sheets. Polymerization can be initiated either by heat or radiation, diffusion of a suitable initiator, or by an organic initiator or catalyst fixed through cation exchange inside the interlayer before the swelling step [15].

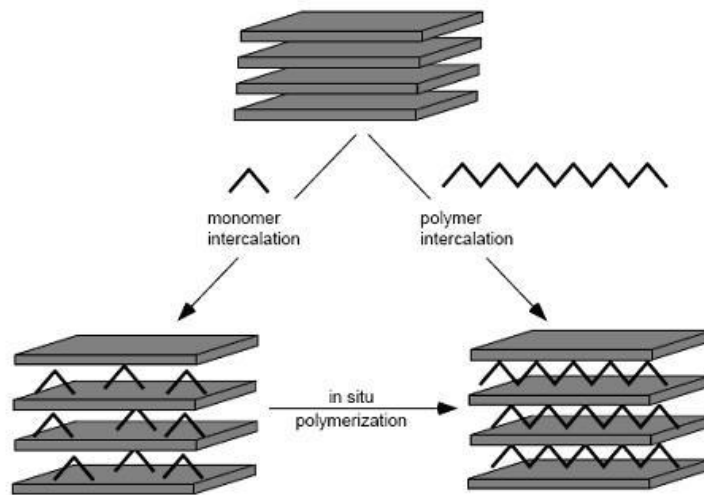


Figure 2.13 : Method for creating intercalated polymer-clay architectures via direct polymer contact and via in-situ polymerization of pre intercalated polymers [15]

2.7 Mechanical Properties of Clay-Containing Polypropylene Nanocomposites

Preparation of the PP-based clay nanocomposites is more complex and interpretation of the mechanical behavior is more difficult. Since PP is immiscible with clays or organoclays, one compatibilizer has to be used at least. Resin is highly crystalline and it concentrates clay platelets in amorph domains, this reduces the interlayer spacing. Clay addition gives relatively similar modulus enhancement in polypropylene and polyamide nanocomposites. The result for good enhancement of a PP-based clay nanocomposite's modulus is low clay concentration, low polymer viscosity, optimized compatibilizer, and long residence time in a compounder. There is a general tendency of (NIISRT) notched izod impact strength at room temperature to increase with $1/E$. However, the data demonstrate that while the modulus depends on the clay content, (NIISRT) notched izod impact strength at room temperature is affected primarily by intercalants and compatibilizers. Thus, the desired rigid and tough Clay Containing Polymeric Nanocomposites might be produced [21].

2.8 Composites Theoretical Models for Modeling Elastic Modulus

Series of micromechanical models have been developed to examine the factorial effects of filler geometry, content and orientation, as well as the property ratio of filler and matrix on the reinforcement and mechanical properties of conventional composites. Besides, the simplified geometry for each component and the

assumption of perfect bonding interfaces, are widely admitted by the material manufacturers and engineers to predict the composite stiffness.

2.8.1 Hui Shia model

Hui Shia model is developed to predict the elastic moduli of composites including unidirectional aligned platelets. It is assumed that there is perfect interfacial bonding between the polymer matrix and platelets, which is given by Longitudinal elastic modulus (E_{11})

$$\frac{E_c}{E_m} = \frac{E_{11}}{E_m} = \frac{1}{1 - (\phi_f/4) [(1/\xi) + 3/(\xi + \Lambda)]} \quad (2.1)$$

Transverse elastic modulus (E_{22})

$$\frac{E_{22}}{E_m} = \frac{1}{1 - (\phi_f/\xi)} \quad (2.2)$$

with

$$\xi = \phi_f + \frac{E_m}{E_f - E_m} + 3(1 - \phi_f) \left[\frac{(1 - g)\alpha^2 - (g/2)}{\alpha^2 - 1} \right] \quad (2.3)$$

and

$$g = (\pi/2)\alpha \quad (2.4)$$

$$\Lambda = (1 - \phi_f) \left[\frac{3(\alpha^2 + 0.25)g - 2\alpha^2}{\alpha^2 - 1} \right] \quad (2.5)$$

Where $\alpha = t / L$ for disk-like platelets ($\alpha \leq 0.1$).

2.8.2 Laminate model

Clay platelets in nanocomposites contain some degree of misalignment and random orientation, however in the conventional composite theories, unidirectionally aligned fillers are normally assumed for simplicity. In the case of completely random orientation in all three orthogonal directions, the approximation equations for elastic moduli of fibre and platelet reinforced composites $E_{\text{ran-3D}}$ based on the laminate theory are derived as

$$E_{\text{ran-3D}}^{\text{fibres}} = 0.184E_{\parallel} + 0.816E_{\perp} \quad (2.5)$$

$$E_{\text{ran-3D}}^{\text{platelets}} = 0.49E_{\parallel} + 0.51E_{\perp} \quad (2.7)$$

where E_{\parallel} and E_{\perp} are the composite moduli in the directions parallel and perpendicular to the principal axis of fillers, respectively. Laminate model helps to predict the elastic moduli of nanocomposites with randomly oriented clay platelets resembling the real morphological structures.

2.8.3 Modified rule of mixture (MROM)

The modified rule of mixture (MROM) is initially introduced to consider the misorientation effect on the imperfectly misaligned random short fibres reinforced into thermoplastics. The similar semi-empirical relationship is further adopted for the flake like fillers in composite materials as

$$E_c = \phi_f E_f (\text{MRF}) + (1 - \phi_f) E_m \quad (2.8)$$

where MRF stands for the Modulus Reduction Factor. MRF stands for less contribution of 2-D flake/platelet fillers to the unidirectional reinforcement. The Modulus Reduction Factor is proposed in two major different forms for flake-like fillers based on Riley's rule and Padawer and Beecher's rule, respectively:

Riley form of MRF:

$$\text{MRF} = 1 - \frac{\ln(u + 1)}{u} \quad (2.9)$$

Padawer and Beecher form of MRF:

$$\text{MRF} = 1 - \frac{\tan hu}{u} \quad (2.10)$$

with

$$u = \frac{1}{\alpha} \sqrt{\frac{\phi_f G_m}{E_f (1 - \phi_f)}} \quad (2.11)$$

where α is the inverse aspect ratio of dispersed fillers and G_m is the shear modulus of the polymer matrix. MRF is between 0.167 and 1 for randomly disposed short fibres. MRF = 0.66 [22] has been studied to predict the tensile moduli of rubber/clay nanocomposites over a wide range of clay volume fractions [23].

2.8.4 Mori Tanaka model

The Mori Tanaka model is based on the principles of Eshelby's inclusion model for predicting an elastic stress field in and around an ellipsoidal filler in an infinite matrix.

The complete analytical solutions for longitudinal E_{11} and transverse E_{22} elastic moduli of an isotropic matrix filled with aligned spherical inclusion are:

$$\frac{E_{11}}{E_m} = \frac{A_0}{A_0 + v_f(A_1 + 2v_0A_2)} \quad (2.12)$$

$$\frac{E_{22}}{E_m} = \frac{2A_0}{2A_0 + v_f(-2A_3 + (1 - v_0)A_4 + (1 + v_0)A_5A_0)} \quad (2.13)$$

where E_m represents the Young's modulus of the matrix, v_f the volume fraction of filler, v_0 the Poisson's ratio of the matrix, parameters, A_0, A_1, \dots, A_5 are functions of the Eshelby's tensor; Young's modulus, Poisson's ratio, filler concentration and filler aspect ratio of filler and matrix [24].

2.8.5. Halpin Tsai Model

Halpin Tsai model is a well-known composites theory in the fibre composites industry to calculate elastic moduli of unidirectional composites as the function of filler volume fraction and aspect ratio. In this model, filler geometries can be different with discontinuous reinforcements such as fibre-like or flake-like fillers. The longitudinal and transverse moduli E_{11} and E_{22} of a composite material in Halpin Tsai model are generally expressed as

$$\frac{E_c}{E_m} = \frac{1 + \zeta\eta\phi_f}{1 - \eta\phi_f} \quad (2.14)$$

$$\eta = \frac{\left(\frac{E_f}{E_m}\right) - 1}{\left(\frac{E_f}{E_m}\right) + \zeta} \quad (2.15)$$

where E_c , E_f and E_m are Young's moduli of composites, fillers and the polymer matrix, respectively. ϕ_f is the filler volume fraction and ζ is a shape parameter depending on the filler geometry and loading direction. $\zeta = 2(l/d)$ for fibres or $2(l/t)$ for disk-like platelets when calculating the longitudinal elastic modulus E_{11} ;

whereas, as an approximation, $\zeta = 2$ for transverse elastic modulus E_{22} due to its relative insensitivity to fibre aspect ratio. L , d and t , are the length, diameter and thickness of dispersed fillers, respectively [23].

2.9 Modeling Elastic Modulus of Polymer Layered Silicate Nanocomposites Using a Modified Halpin Tsai Micromechanical Model

Halpin and Tsai developed a well-known composite theory for predicting the stiffness of unidirectional composites as a function of aspect ratio. This theory is based on the early micromechanical works of Hermans and Hill. Hermans generalized the form of Hill's self-consistent theory by considering a single fiber encased in a cylindrical shell of the matrix. This is embedded in an infinite medium that is supposed to have the average properties of the composite. Halpin and Tsai reduced Herman's results into a simpler analytical form. This form can be adapted to different reinforcement geometries, including discontinuous filler reinforcement.

Number of assumptions are supposed to exist in this approach: (i) the filler and matrix are linearly elastic, isotropic, and firmly bonded, (ii) the filler is perfectly aligned, asymmetric, and uniform in shape and size, and (iii) particle–particle interactions are not explicitly considered.

In all composite theories, the properties of the matrix and filler are considered to be identical to those of the pure components. For this reason, numerous complexities arise when comparing the composite theory to the experimental composite data, especially for polymer-layered silicate nanocomposites. Calculated and observed properties are affected from choice of composite theory in addition to physical differences between the theory and the experiment.

The Halpin Tsai model is chosen in this work because of its effectiveness in calculating the stiffness of glass fiber reinforced composites. This model is adaptable for different filler geometries, particularly disks, In literature, there are relatively few reports that deal specifically with nanocomposites.

Halpin Tsai model provides effective composite theoretical analysis in the fibre composites industry to calculate the elastic modulus of a unidirectional composite as a function of filler aspect ratio and volume fraction. It works with different reinforcement geometries of discontinuous fillers such as fibre-like or flake-like

fillers. The Young's modulus of a composite material in Halpin Tsai model is written as

$$\frac{E_c}{E_m} = \frac{1 + \zeta\eta\phi_f}{1 - \eta\phi_f} \quad (2.16)$$

$$\eta = \frac{\frac{E_f}{E_m} - 1}{\frac{E_f}{E_m} + \zeta} \quad (2.17)$$

E_c = Young's modulus of composites

E_f = Young's modulus of fillers

E_m = Elastic modulus of polymer matrix

ϕ_f = Filler volume fraction

ζ = Shape parameter depending on the filler geometry and loading direction

$\zeta = 2(l/d)$ for fibres

$\zeta = 2(l/t)$ for disk-like platelets

l = Length of dispersed filler

d = Diameter of dispersed filler

t = Thickness of dispersed filler

Since 2-D disk-like clay platelets decrease the unidirectional reinforcement in comparison with 1-D fibre-like fillers, a modulus reduction factor (MRF) for platelet fillers is thus introduced in the modified Halpin Tsai model as follows [25]:

$$\frac{E_c}{E_m} = \frac{1 + \zeta(\text{MRF})\eta\phi_f}{1 - \eta\phi_f} \quad (2.18)$$

Predicted modulus by Halpin Tsai equation is higher than the experimental data in rubber-clay composites. Contribution of plate-like clay (two dimension) to modulus is less than a fiber like dispersed phase (one dimension). It has been observed that the morphology difference between the plate-like filler and the fiber-like filler phase, which is neglected in the theories of the modulus prediction, should be taken into account. As a result, the modulus reduction factor (MRF) for the platelet-like fillers has been included in Halpin Tsai equations. Since MRF is related to the morphology of the filler, MRF should appear together with the aspect ratio. Improvement in the predicting ability of the Halpin Tsai equation is to be expected after including MRF.

When the predicted values at filler volume concentrations are less than 6%, we choose MRF to be 0.66 [22] so that predicted values fit experimental data. In the following study, we choose the MRF value of 0.66 [22][29].

The clay particles or their layers are incorporated into a polymer matrix so that they form an organic/inorganic composite. The polymer/clay composites can be divided into four categories depending on the concentration of clay, degree of separation, and distribution of layers of clay in composite. (Figure 2.13)

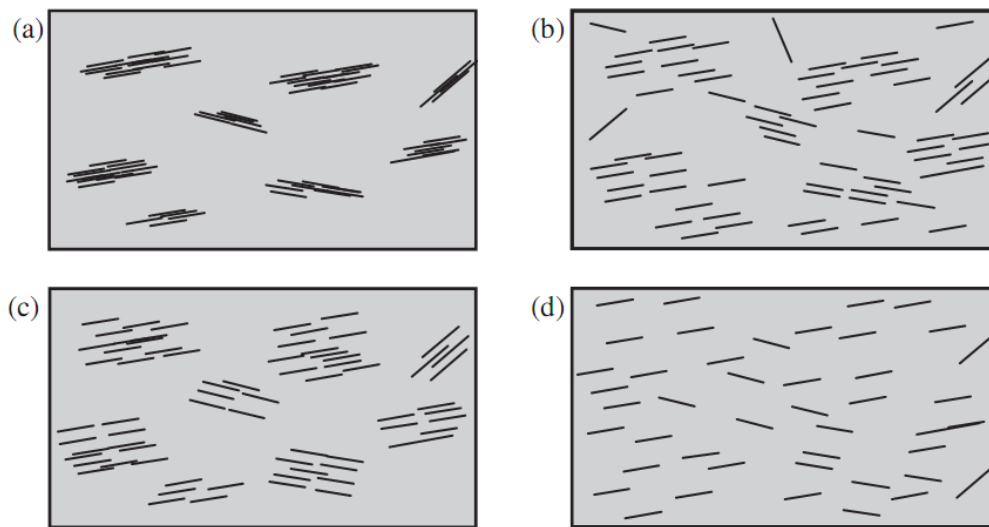


Figure 2.14 : Schematic illustrations of types of polymer/clay composites [26]:

- (a) conventional miscible composite
- (b) partially intercalated and exfoliated nanocomposite
- (c) fully intercalated nanocomposite
- (d) fully exfoliated polymer–clay nanocomposite

The clay interlayer spacing is fixed in an intercalated nanocomposite. The average gallery height is determined by the clay silicate loading in an exfoliated nanocomposite. In most commonly occurring cases of polymer/clay nanocomposites, the exfoliated clay layers and the intercalated clusters are randomly distributed in the polymer matrix (Figure 2.13(b)).

Traditional mechanical models can not well predict increase in stiffness, because no ideal conditions are achieved in terms of the full exfoliation, dispersion, and orientation of the clay platelets. Partial exfoliation and intercalation and randomly dispersed exfoliated platelets and intercalated clusters can be observed in current manufacturing processes. Exfoliated clay nanolayers can be considered as fillers with high aspect ratios with a random or preferred orientation. Intercalated clusters can differ in thickness and layer spacing (d-spacing) depending on the degree of

intercalation. The intercalation process produces a second group of fillers with physical sizes in the micro and sub-micro scale. The clusters are highly anisotropic due to the thermal and elastic mismatch between the matrix and nanoclay phases.

Full exfoliate or full intercalate status cannot be achieved in the current industrial nanocomposite fabrication process. Polymer/clay nanocomposites in this study considers the existence of both intercalation and exfoliation. The fully exfoliate (Figure 2.13(d)) or fully intercalate (Figure 2.13(c)) status can be treated as an extreme case for the model.

2.9.1 Effective representation of the nanoclay

Further development and optimization of polymer/MMT materials from the mechanical point of view require study of models for the measurement and prediction of properties, such as stiffness, strength, fracture toughness, and the coefficient of thermal expansion. Studies have been made to develop & apply expressions for the effective moduli of unidirectional nanocomposites with dispersed and parallel flake-like fillers. These simplified models assume complete exfoliation of the clay layers, full dispersion, and uniform orientation. These idealized models are not in agreement with the experimental results. Differences are attributed to the natural complexity of the nanocomposite structure, such as debonding between clay nanolayers and the polymer matrix. As a result, it is necessary to introduce the concept of the ‘effective particle’.

2.9.1.1 Concept of the effective particle

Models for the macroscopic properties of composite materials are on the ‘particle’ and the ‘matrix’. The total three dimensional volume of the composite is divided into the ‘particle domain’ and the ‘matrix domain,’ as shown in Figure 2.13(a). Each domain is then treated as a homogeneous material, with certain elastic properties. However, a clearly defined ‘particle domain’ does not exist in the intercalated polymer/clay nanocomposites. Here, the concept of indicating the three dimensional domain of the ‘effective particle’ has been accepted, similar to that proposed in Brune and Bicerano. The ‘effective particle’ is identified by a well-defined spatial volume, occupied by both the silicate layers and the interlayer galleries. Mechanical description of the silicate layers, which can universally represent conventional, intercalated, and exfoliated fillers, is has importance in this study.

Surrounding the exterior silicate layers is a special morphology material composed of some blend of surfactants and matrix polymer chains, which rapidly undergoes transition to a 100% matrix material with increasing distance from the particle. For the present purpose, these special regions and features are neglected, and they are simply included within the matrix volume and matrix properties. The proposed approach can be obviously extended to account for these features within the definition of the ‘effective particle’.

Table 2.6: Characteristic values of the polymer-clay structure – descriptive [26]

Symbol	Characteristic Parameter	Typical Value(nm)
L_p	Length of the dispersed clay particles	130-180
ζ_p	Correlation between particles (interparticle spacing)	40-60
t_p	Thickness of the clay particles	7-9
$d_{(001)}$	Interlayer spacing of the plane platelet in intercalated clay	3
$d_{lamellae}$	Average lamellae thickness of polymer matrix crystallite	7
$L_{lamellae}$	Long-period lamellae thickness of polymer crystallite	15

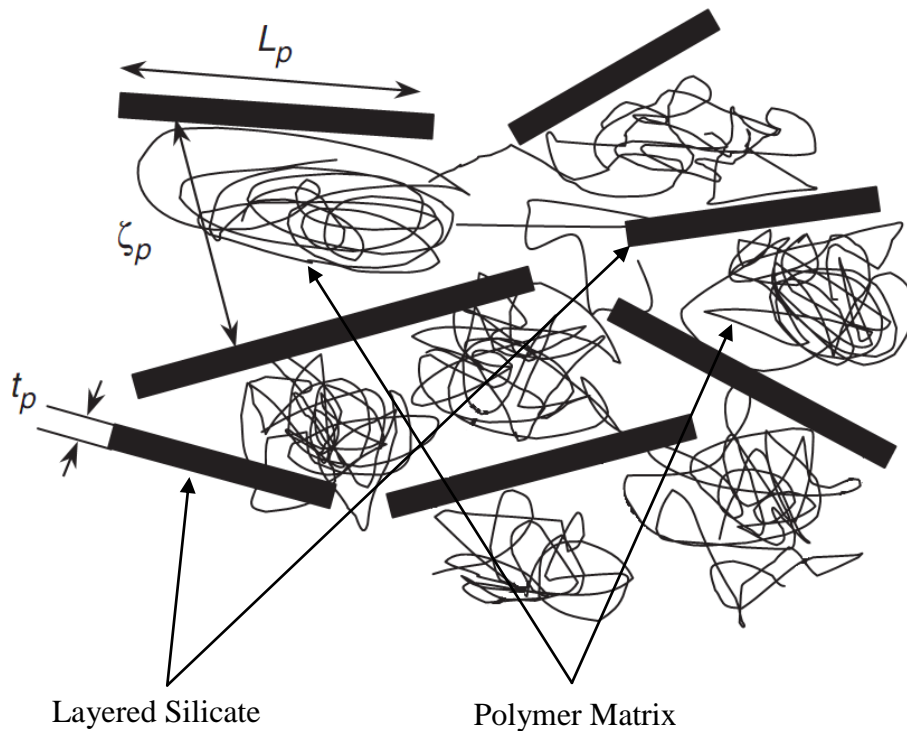


Figure 2.15 : Schematic of the polymer-clay morphology and characteristic parameters [26]

The nanocomposite is supposed to have two homogeneous phases: polymer matrix and high aspect ratio clay particles. Here, analytical predictions of the overall composite elastic modulus are studied. Stiffness improvement mechanisms are summarized using simple, idealized numerical solutions. These models can be modified and applied to polymer/clay nanocomposites, where the intercalated nanoclay is a heterogeneous laminate-like structure. This structure is modeled with reasonable homogenization of the geometry and properties of the ‘effective particle’.

2.9.1.2 Parallel platelet system

Montmorillonite clay has a larger surface area (up to 750 m²/g) available for potential contact with the polymer. Aim is to achieve good dispersion and exfoliation of the clay so that the high aspect ratio and surface area of the clay can be obtained. Natural clays exist as ‘tactoids’ or stacks of platelets, as shown in Figure 2.15.

The polymer matrix and clay nanolayers were assumed to be isotropic and the properties of intercalated clay clusters were computed by supposing them as a system of parallel nanolayers. The internal structure of an intercalated nanoclay particle is simplified as a multi-layer parallel platelet stack containing N single silicate sheets with a uniform interlayer spacing $d_{(001)}$ and layer thickness d_s . N is the number of

silicate sheets, as shown in Figure 2.16 . The very close sheets are separated in a ‘gallery layer’ made of both surfactants and polymer matrix chains that have penetrated the intersilicate layers during various stages of synthesis and processing. The particle thickness ‘t’ can be related to the internal structural parameters N and $d_{(001)}$ through

$$t = (N - 1)d_{(001)} + d_s \quad (2.19)$$

where d_s is the thickness of the silicate sheet. A similar approach is used in, where effective particle thickness is expressed in terms of multiples of sheet thickness and gallery thickness. There are some uncertain points in assigning a precise value to thickness for nanoparticles of atomic level thickness as nanoclay sheets, especially with regard to providing an accurate representation of mechanical properties using continuum level models.

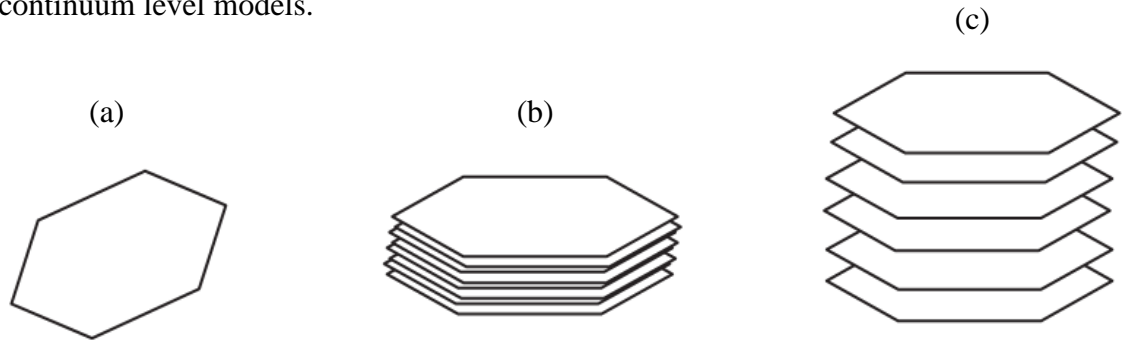


Figure 2.16 : Simplified schematic showing (L to R) (a) an individual clay platelet (b) a compact clay tactoid (c) a swollen clay tactoid [26]

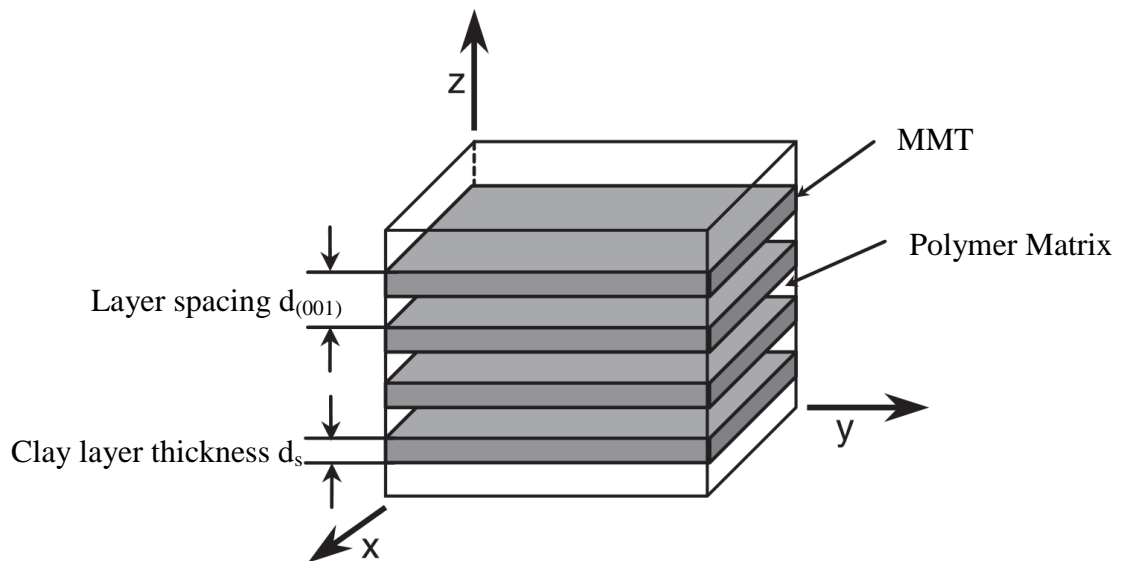


Figure 2.17 : A representative element of an intercalated cluster of clay nanolayers assumptions as a parallel platelet system [26]

2.9.1.3 Properties of the effective clay particle

TX_N is the clay structure parameter, which expressed as the number of silicate sheets, (N) per unit particle thickness (t) (refer to Figure 2.16 for the meaning of the other parameters):

$$X_N = \frac{N}{t} = \frac{N}{(N-1)d_{(001)} + d_s} \quad (2.20)$$

which can alternatively be expressed as the volume fraction of silicate in the effective particle as a dimensionless quantity X:

$$X = \frac{V_{\text{silicate}}}{V_p} = \frac{Nd_s}{(N-1)d_{(001)} + d_s} = \frac{1}{(1-1/N)(d_{(001)}/d_s) + 1/N} \quad (2.21)$$

V_{silicate} : volume of silicate sheets in stack

V_p : volume of effective particle

X is a function of two internal parameters of the nanoclay particle

N: number of silicate sheets

$d_{(001)}/d_s$: the relative inter-layer swelling

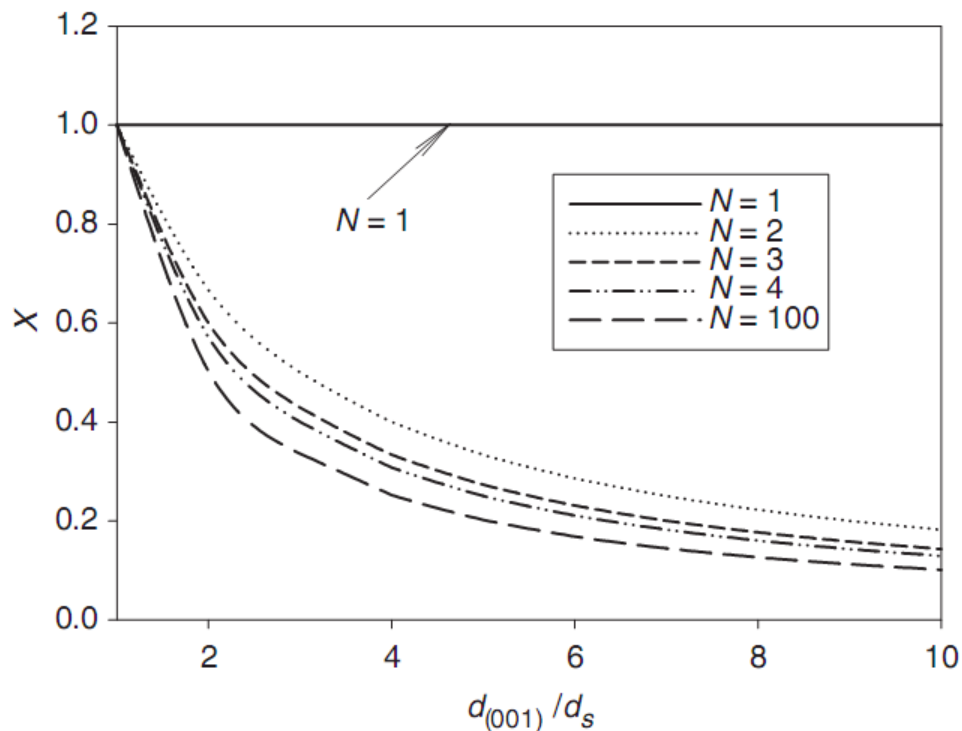


Figure 2.18 : Dependence of particle silicate volume fraction X on clay structural parameters N and $d_{(001)}/d_s$ [26]

Figure 2.17 shows a decrease in the silicate volume fraction X with increasing $d_{(001)}/d_s$ for different N values. The observation that the case $N=1$ differs from the others; ($N>1$) suggests that there is a significant distinction in structure-related effective particle properties between exfoliated systems and intercalated systems. Similar effects on X_N are to be expected since $X_N = X/d_s$.

The effective particle is ‘equivalent’ to the multilayer stack in the sense that it has the same L/t , f_p , and overall mechanical properties as the discrete stack. The aspect ratio L/t can be calculated as:

$$\frac{L}{t} = \frac{L}{(N-1)d_{(001)} + d_s} \quad (2.22)$$

Equation (2.22) can be further written in terms of X_N and N as:

$$\frac{L}{t} = \left(\frac{L}{N}\right) X_N \quad (2.23)$$

The modified composite-based micromechanical models can provide good predictions of the overall modulus of the polymer/clay nanocomposites. The intercalated nanoclay, modeled as a multilayer stack with N silicate sheets and an interlayer spacing of $d_{(001)}$, can be represented as a homogeneous ‘particle’, which possesses the same three dimensional domain occupied by both the silicate layers and the interlayer galleries. A careful correlation between the characteristic clay structural parameters (N , $d_{(001)}$) and the clay weight fraction (w_f), and the conventional micromechanical model parameters (particle volume fraction ϕ and particle aspect ratio ‘ l/t ’) was established [26].

3. EXPERIMENTAL PART

3.1 Chemicals Used

3.1.1 Polyethylene, Polypropylene (PE, PP)

Commercial polyolefin samples of polyethylene and polypropylene with different molecular weights and properties for determination of elastic modulus of polymeric nanocomposites with Halpin Tsai micromechanical modeling.

3.1.1.1 Low Density Polyethylene (LDPE)

LDPE was obtained from PETKIM Petrochemical Holding (G03-5).

3.1.1.2 Linear Low Density Polyethylene (LLDPE)

LLDPE was obtained from Exxon Corp. Density of LLDPE is 0.91 - 0.925 g/cm³ [28].

3.1.1.3 Metallocene Linear Low Density Polyethylene (mLLDPE)

mLLDPE, whose density 0.927g/cm³, was obtained from Exxon Mobile Company [27].

3.1.1.4 Capilene SB56 (Cp)

Impact copolymer was obtained from Carmel olefins. Capilene SB56 is a low melt flow rate impact copolymer. Capilene SB56's Melt flow index (MFI) is 0.35 g/10 min.; flexural modulus: 1050 MPa [29].

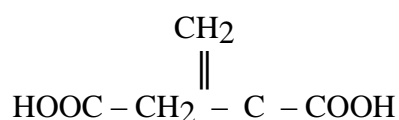
3.1.1.5 Buplen 6531 (Bp)

PP homopolymer was obtained from Lukoil Bulgaria Ltd. Buplen 6531's MFI is 3.0 to 5.0 g/10 min, specific gravity: 0.898-0.905 g/cm³; flexural modulus >1100 MPa [29].

3.1.1.6 Petoplen MH-418 (MH-418)

Isotactic polypropylene (MH-418) was obtained from PETKIM Petrochemical Co. Its specific gravity is 0.905 g/cm³; MFI : 4.0 to 6.0 g/10 min.; flexural modulus: 1420 MPa [29].

3.1.2 Itaconic Acid (IA)



Systematic name, 2-methylene succinic acid, was the product of Fluka A. G. With a 99% purification, was used without any purification procedure. (m.p. = 165- 167 °C).

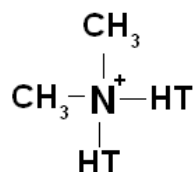
3.1.3 Montmorillonite (MMT)

3.1.3.1 Sodium Montmorillonite (Na-MMT)

The nanofiller (Nanofil 757), sodium-montmorillonite (Na-MMT), used in the preparation of organoclay was received from Süd-Chemi Inc. It is a highly purified natural Na-MMT with cation-exchange capacity (CEC) of 0.080 meq/g, average particle size < 10 meq, and bulk density of approximately 2.6 g/mL [27][28].

3.1.2.2 Modified MMT

The layered silicate was Nanofil 8 which is an organically modified nanodispersible layered silicate based on a natural bentonite. The surface treatment is a dimethyl, di(hydrogenated tallow) alkyl ammonium salt [29].



3.1.4 Dodecyl amine (DDA)

With the formula C₁₂H₂₇N dodecyl amine is an alifatic amine and its molecular weight is 185.36 g/mol. It was received from "Merck" and was used without any purification (MP = 25-28 °C) [28].

3.1.5 Hexadecyl amine (HDA)

With the formula $C_{16}H_{35}N$ hexadecyl amine is an alifatic amine and its molecular weight is 241.46 g/mol. It was received from "Merck" and was used without any purification (MP = 43-46 °C) [28].

3.1.6 Octadecyl amine (ODA)

$C_{18}H_{39}N$ octadecyl amine is an alifatic amine and its molecular weight is 269.52 g/mol. It was received from "Merck" and was used without any purification (MP = 52-56 °C) [28].

3.2 Preparation of Organoclays

DDA, HDA, and ODA modified clays were prepared the procedure given in the literature [30].

3.3 Preparation of Polymer Nanocomposites

Single step melt mixing method was used to prepare PNCs for all samples. For this purpose, optimization conditions were determined at different temperatures, cycling time and rotational speed for single step melt mixing in MiniLab twin screw extruder. During the optimization, the important criteria were to prevent the degraded polymer structure and shark skin effect, and to provide the homogeneity of polymer nanocomposites.

For LDPE and LLDPE nanocomposite preparation, optimization conditions were determined as 177 °C set temperature, 87 rpm screw speed with 2 min. cycling time [28].

For preparation mLLDPE nanocomposites, optimized operating conditions are 160 °C extruder temperature, 90 rpm screw speed, 2 min. cycle time [27].

For PPNC samples, optimized conditions were determined as 216 °C extruder temperature, 100 rpm screw speed, 2 min cycle time.

In the previous works, to determine the influence of the cycle time on homogeneity, surface appearance and output, the experiments were done within the range of 2-7 min [29].

3.4 Calculation Process Using Modified Halpin Tsai Micromechanical Modeling

In this study, Modified Halpin Tsai model was used to predict “l/t” values of synthesized polyolefins.

$$\eta = \frac{\frac{E_f}{E_m} - 1}{\frac{E_f}{E_m} + \zeta} \quad (2.17)$$

$$\frac{E_c}{E_m} = \frac{1 + \zeta(\text{MRF})\eta\phi_f}{1 - \eta\phi_f} \quad (2.18)$$

E_c = Young's modulus of composites

E_f = Young's modulus of fillers

E_m = Elastic modulus of polymer matrix

ϕ_f = Filler volume fraction

ζ = Shape parameter depending on the filler geometry and loading direction

$\zeta = 2(l/d)$ for fibres

$\zeta = 2(l/t)$ for disk-like platelets

l = Length of dispersed filler

d = Diameter of dispersed filler

t = Thickness of dispersed filler

Initially ϕ_f (filler volume fraction) is calculated from density and mass of ingredients of nanocomposites.

Since we regard montmorillonite as fillers in Halpin Tsai approach, we can calculate filler volume fraction with the help of TGA analysis of components. From TGA analysis we obtain montmorillonite content of organoclays.

Firstly, we divide organoclay mass by MMT density. In order to calculate volume of montmorillonite content, we multiply result with MMT weight percentage data that we obtained from TGA analysis.

Secondly, we calculate total volume of nanocomposite by summing volume of each ingredient by dividing mass over density.

Thirdly, we divide volume of montmorillonite by total volume, from which we obtain Φ_f (filler volume fraction).

MRF value is found to be 0.66 [22].

Our scope is to predict “ l/t ” values from overall equation; ζ is obtained by multiplying “ l/t ” by 2.

We have the ratio of Young modulus of PNC matrix elastic modulus. From this value and ζ , we calculate η and use in main equation.

$$\eta = \frac{\frac{E_f}{E_m} - 1}{\frac{E_f}{E_m} + \zeta} \quad (2.17)$$

We place composite modulus that we obtained from experiment and polymer matrix modulus that we obtained from literature in main halpin tsai equation. With the given values we calculated, it's possible to predict exfoliated or intercalated structure by “ l/t ” [29].

3.5 Calculations Using Modified Halpin Tsai Micromechanical Modeling

In order to calculate “ l/t ” ratios for the PO NCs, the following parameters were found and used in the equations 2.17 and 2.18.

3.5.1 Calculation of “ l/t ”

In these calculations, we need to use the MRF, E_c , E_m , E_f , Φ_f , density of montmorillonite, pure polymers, calculate “ l/t ” by using Halpin Tsai equation.

3.5.1.1 MRF

MRF value is chosen to be 0.66 in all calculations [22].

3.5.1.2 Young modulus of polymeric nanocomposites (E_c)

Table 3.1: Young modulus of used polymer nanocomposites [27] [28] [29]

Polymer Nanocomposites	Young Modulus (MPa)
LDPE-IA-O _{DDA} 5-C5	170
LDPE-IA-O _{DDA} 5-C10	284.5
LDPE-IA-O _{DDA} 5-C15	290

LDPE- MMI-O _{DDA} 5-C5	242.3
LDPE- MMI-O _{DDA} 5-C10	295
LDPE- MMI-O _{DDA} 5-C15	343.8
LDPE-IA-O _{HDA} 5-C5	327.5
LDPE-IA-O _{HDA} 5-C10	393.3
LDPE-IA-O _{HDA} 5-C15	490
LDPE- MMI-O _{HDA} 5-C5	297.6
LDPE- MMI-O _{HDA} 5-C10	355.3
LDPE- MMI-O _{HDA} 5-C15	465
LDPE-IA-O _{ODA} 5-C5	283.3
LDPE-IA-O _{ODA} 5-C10	340
LDPE-IA-O _{ODA} 5-C15	378.3
LDPE- MMI-O _{ODA} 5-C5	253.3
LDPE- MMI-O _{ODA} 5-C10	298
LDPE- MMI-O _{ODA} 5-C15	345
LLDPE-IA-O _{DDA} 5-C5	310
LLDPE-IA-O _{DDA} 5-C10	375
LLDPE-IA-O _{DDA} 5-C15	400
LLDPE-MMI-O _{DDA} 5-C5	295
LLDPE-MMI-O _{DDA} 5-C10	340
LLDPE-MMI-O _{DDA} 5-C15	390
LLDPE-IA-O _{HDA} 5-C5	320
LLDPE-IA-O _{HDA} 5-C10	368
LLDPE-IA-O _{HDA} 5-C15	400
LLDPE-MMI-O _{HDA} 5-C5	305.4
LLDPE-MMI-O _{HDA} 5-C10	358
LLDPE-MMI-O _{HDA} 5-C15	395
LLDPE-IA-O _{ODA} 5-C5	266
LLDPE-IA-O _{ODA} 5-C10	387
LLDPE-IA-O _{ODA} 5-C15	518
LLDPE-MMI-O _{ODA} 5-C5	266
LLDPE-MMI-O _{ODA} 5-C10	350
LLDPE-MMI-O _{ODA} 5-C15	520
mLLDPE- O _{ODA} 5 - C 5	418.7
mLLDPE - O _{ODA} 5 - C 10	423
mLLDPE - O _{ODA} 5 - C 15	372.8

mLLDPE - O _{ODA} 5 - C 20	277.4
PP _{CAP} - O _{NANOFIL8} 3 - C10	980
PP _{CAP} - O _{NANOFIL8} 5-C15	1300
PP _{BUP} - O _{NANOFIL8} 3- C10	1120
PP _{BUP} - O _{NANOFIL8} 5- C15	1210
PP _{MH418} - O _{NANOFIL8} 3- C10	1210
PP _{MH418} - O _{NANOFIL8} 5- C 15	1280

3.5.1.3 Young modulus of pure polymers (E_m)

Table 3.2: Young modulus of used pure polymers [27] [28] [29]

Polymer	Young Modulus (MPa)
LDPE	167
LLDPE	215
mLLDPE	365.7
Capilene SB56	1080
Buplen 6531	925
Petoplen MH-418	1120

3.5.1.4 Young modulus of Montmorillonite (E_f)

Young Modulus of Montmorillonite is used as 170000 MPa [32].

3.5.1.5 MMT content in organoclays and filler volume fraction (Φ_f)

1000 kg of material is valued to be used virtually to determine filler volume fraction.

The equation for calculation of filler volume fraction (Φ_f) is given as follows:

$$\phi_f = \frac{\left(\frac{\text{Mass of Organoclay} * \text{MMT Content}}{\text{Density of MMT Content}} \right)}{\left(\frac{\text{Mass of organoclay}}{\text{Density of organoclay}} \right) + \left(\frac{\text{Mass of Compatibilizer}}{\text{Density of Compatibilizer}} \right) + \left(\frac{\text{Mass of polymer matrix}}{\text{Density of polymer matrix}} \right)} \quad (3.1)$$

Table 3.3: MMT contents of organoclay used in this work [31] [32] [33] [41]

Polymer Matrix Used in Calculation	Organoclay	MMT Content of Organoclay (%)
LDPE	O _{DDA}	62
LDPE	O _{HDA}	79
LDPE	O _{ODA}	74
LLDPE	O _{DDA}	62
LLDPE	O _{HDA}	79
LLDPE	O _{ODA}	74
mLLDPE	O _{ODA}	74
PP - Capilene	Nanofil 8	57

PP - Buplen 6531	Nanofil 8	57
PP - Petoplen MH-418	Nanofil 8	57

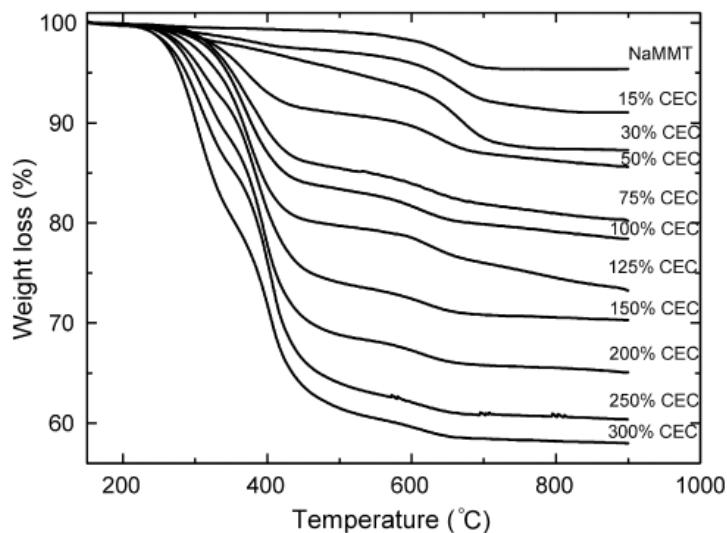


Fig. 3.1 : TGA curves of natural and organomodified montmorillonites with various concentrations of hexadecylamine (related to the clay CEC) [31]

From graph above, we reference %100 CEC and measure weight loss content from graph. Determined MMT content is %79 [31].

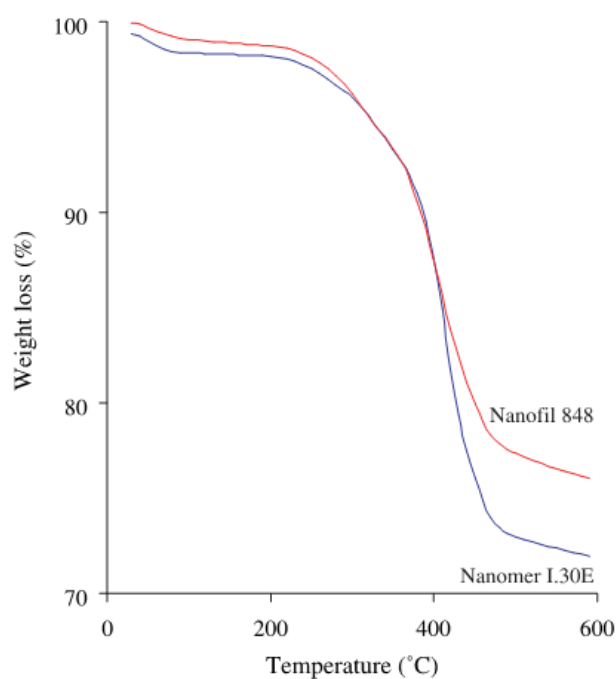


Fig. 3.2 : TGA data from primary alkyl ammonium surfactants [32]

The weight loss recorded for Nanomer I.30E was 26 % [32]. The loss of ignition of Cloisite® 20A is %38. The MMT content of O_{dda} is 62% [41]. The loss of ignition of Nanofil® 8 is 43% [33]. We use these values to calculate montmorillonite volume fraction.

Table 3.4: Calculated filler volume fraction of the samples [27] [28] [29].

Polymeric Nanocomposites	Φf –Filler Volume Fraction	Organo- Clay Content (%)	Compa- tibilizer Content (%)	Polymer Matrix Content (%)
LDPE-IA-O _{DDA} 5-C5	0.011062035	5	5	90
LDPE-IA-O _{DDA} 5-C10	0.011062035	5	10	85
LDPE-IA-O _{DDA} 5-C15	0.011062035	5	15	80
LDPE- MMI-O _{DDA} 5-C5	0.011062035	5	5	90
LDPE- MMI-O _{DDA} 5-C10	0.011062035	5	10	85
LDPE- MMI-O _{DDA} 5-C15	0.011062035	5	15	80
LDPE-IA-O _{HDA} 5-C5	0.014079687	5	5	90
LDPE-IA-O _{HDA} 5-C10	0.014079687	5	10	85
LDPE-IA-O _{HDA} 5-C15	0.014079687	5	15	80
LDPE- MMI-O _{HDA} 5-C5	0.014079687	5	5	90
LDPE- MMI-O _{HDA} 5-C10	0.014079687	5	10	85
LDPE- MMI-O _{HDA} 5-C15	0.014079687	5	15	80
LDPE-IA-O _{ODA} 5-C5	0.013179744	5	5	90
LDPE-IA-O _{ODA} 5-C10	0.013179744	5	10	85
LDPE-IA-O _{ODA} 5-C15	0.013179744	5	15	80
LDPE- MMI-O _{ODA} 5-C5	0.013179744	5	5	90
LDPE- MMI-O _{ODA} 5-C10	0.013179744	5	10	85
LDPE- MMI-OC _{ODA} 5-C15	0.013179744	5	15	80
LLDPE-IA-O _{DDA} 5 –C5	0.011085363	5	5	90
LLDPE-IA-O _{DDA} 5-C10	0.011085363	5	10	85
LLDPE-IA-O _{DDA} 5-C15	0.011085363	5	15	80
LLDPE-MMI-O _{DDA} 5-C5	0.011085363	5	5	90
LLDPE-MMI-O _{DDA} 5-C10	0.011085363	5	10	85
LLDPE-MMI-O _{DDA} 5-C15	0.011085363	5	15	80
LLDPE-IA-O _{HDA} 5-C5	0.014109346	5	5	90
LLDPE-IA-O _{HDA} 5-C10	0.014109346	5	10	85
LLDPE-IA-O _{HDA} 5-C15	0.014109346	5	15	80
LLDPE-MMI-O _{HDA} 5-C5	0.014109346	5	5	90
LLDPE-MMI-O _{HDA} 5-C10	0.014109346	5	10	85
LLDPE-MMI-O _{HDA} 5-C15	0.014109346	5	15	80
LLDPE-IA-O _{ODA} 5-C5	0.013207489	5	5	90
LLDPE-IA-O _{ODA} 5-C10	0.013207489	5	10	85
LLDPE-IA-O _{ODA} 5-C15	0.013207489	5	15	80
LLDPE-MMI-O _{ODA} 5-C5	0.013207489	5	5	90
LLDPE-MMI-O _{ODA} 5-C10	0.013207489	5	10	85
LLDPE-MMI-O _{ODA} 5-C15	0.013207489	5	15	80
mLLDPE- O _{ODA} 5 - C 5	0.013235230	5	5	90
mLLDPE - O _{ODA} 5 - C 10	0.013235230	5	10	85
mLLDPE - O _{ODA} 5 - C 15	0.013235230	5	15	80

mLLDPE - O _{ODA} 5 - C 20	0.013235230	5	20	75
PP _{CAP} - O _{NANOFIL8} 3 - C10	0.005920595	3	10	87
PP _{CAP} - O _{NANOFIL8} 5-C15	0.009959508	5	15	80
PP _{BUP} - O _{NANOFIL8} 3- C10	0.005894859	3	10	87
PP _{BUP} - O _{NANOFIL8} 5- C15	0.009916710	5	15	80
PP _{MH 418} - O _{NANOFIL8} 3- C10	0.005920595	3	10	87
PP _{MH418} - O _{NANOFIL8} 5- C 15	0.009959508	5	15	80

3.5.1.6 Density of clay

In literature, density of MMT is found as 2650 kg/m³[35].

3.5.1.7 Densities of pure polymers

Table 3.5: Densities of pure polymers [27][28][29].

Polymer	Density (kg/m ³)
LDPE	923
LLDPE	925
mLLDPE	927
Capilene SB56	901
Buplen 6531	905
Petoplen MH-418	905

3.5.1.8 Densities of used organoclays

Table 3.6: Densities of used organoclays [41][33][36].

Organoclay	Density (kg/m ³)
MMT - DDA	1770
MMT - HDA	1700
MMT - ODA	1660
Nanofil 8	1660

3.5.1.9 Densities of compatibilizers

Density of compatibilizers are used same with pure polymer matrixes since IA and MMI is grafted onto main matrix in less than %0.002 percent in mass.

3.5.2 Calculated values “l/t”

In Halpin Tsai Equations

$$\zeta = 2(l/t)$$

“l/t” is length over thickness ratio of tactoids, we can derive intercalated or exfoliated structure from these data.

Table 3.7: Calculated “1/t” values of samples.

Polymeric Nancomposites	1/t
LDPE-IA-O _{DDA} 5-C5	0.46
LDPE-IA-O _{DDA} 5-C10	51.85
LDPE-IA-O _{DDA} 5-C15	54.59
LDPE- MMI-O _{DDA} 5-C5	31.73
LDPE- MMI-O _{DDA} 5-C10	57.09
LDPE- MMI-O _{DDA} 5-C15	82.82
LDPE-IA-O _{HDA} 5-C5	55.97
LDPE-IA-O _{HDA} 5-C10	83.11
LDPE-IA-O _{HDA} 5-C15	128.18
LDPE- MMI-O _{HDA} 5-C5	44.44
LDPE- MMI-O _{HDA} 5-C10	67.12
LDPE- MMI-O _{HDA} 5-C15	115.88
LDPE-IA-O _{ODA} 5-C5	42.09
LDPE-IA-O _{ODA} 5-C10	65.76
LDPE-IA-O _{ODA} 5-C15	82.94
LDPE- MMI-O _{ODA} 5-C5	30.35
LDPE- MMI-O _{ODA} 5-C10	48.04
LDPE- MMI-O _{ODA} 5-C15	67.94
LLDPE-IA-O _{DDA} 5 - C5	31.55
LLDPE-IA-O _{DDA} 5-C10	56.93
LLDPE-IA-O _{DDA} 5-C15	67.52
LLDPE-MMI-O _{DDA} 5-C5	26.103
LLDPE-MMI-O _{DDA} 5-C10	42.903
LLDPE-MMI-O _{DDA} 5-C15	63.23
LLDPE-IA-O _{HDA} 5-C5	26.91
LLDPE-IA-O _{HDA} 5-C10	40.92
LLDPE-IA-O _{HDA} 5-C15	50.79
LLDPE-MMI-O _{HDA} 5-C5	22.83
LLDPE-MMI-O _{HDA} 5-C10	37.92
LLDPE-MMI-O _{HDA} 5-C15	49.22
LLDPE-IA-O _{ODA} 5-C5	13.13
LLDPE-IA-O _{ODA} 5-C10	50.44
LLDPE-IA-O _{ODA} 5-C15	99.48
LLDPE-MMI-O _{ODA} 5-C5	13.13
LLDPE-MMI-O _{ODA} 5-C10	38.32
LLDPE-MMI-O _{ODA} 5-C15	100.31
mLLDPE- O _{ODA} 5 - C 5	7.72

mLLDPE - O _{ODA} 5 - C 10	8.43
mLLDPE - O _{ODA} 5 - C 15	0.34
mLLDPE - O _{ODA} 5 - C 20	0.01
PP _{CAP} - O _{NANOFIL8} 3 - C10	0.01
PP _{CAP} - O _{NANOFIL8} 5-C15	18.31
PP _{BUP} - O _{NANOFIL8} 3- C10	37.41
PP _{BUP} - O _{NANOFIL8} 5- C15	30.54
PP _{MH418} - O _{NANOFIL8} 3- C10	11.03
PP _{MH418} - O _{NANOFIL8} 5- C 15	11.77

4. CONCLUSION AND RECOMMENDATIONS

Halpin Tsai model provides effective composite theoretical analysis in the fibre composites industry to calculate the elastic modulus of a unidirectional composite as a function of filler aspect ratio and volume fraction. It works with different reinforcement geometries of discontinuous fillers such as fibre-like or flake-like fillers. The Young's modulus of a composite material in Halpin Tsai model is written as

$$\frac{E_c}{E_m} = \frac{1 + \zeta\eta\phi_f}{1 - \eta\phi_f} \quad (2.16)$$

$$\eta = \frac{\frac{E_f}{E_m} - 1}{\frac{E_f}{E_m} + \zeta} \quad (2.17)$$

E_c = Young's modulus of composites

E_f = Young's modulus of fillers

E_m = Elastic modulus of polymer matrix

ϕ_f = Filler volume fraction

ζ = Shape parameter depending on the filler geometry and loading direction

$\zeta = 2(l/d)$ for fibres

$\zeta = 2(l/t)$ for disk-like platelets

l = Length of dispersed filler

d = Diameter of dispersed filler

t = Thickness of dispersed filler

Since 2-D disk-like clay platelets decrease the unidirectional reinforcement in comparison with 1-D fibre-like fillers, a modulus reduction factor (MRF) for platelet fillers is thus introduced in the modified Halpin Tsai model as follows [25]:

$$\frac{E_c}{E_m} = \frac{1 + \zeta(\text{MRF})\eta\phi_f}{1 - \eta\phi_f} \quad (2.18)$$

4.1 Calculation of “l/t” Values of Experimental Young Modulus Data

Calculations that were given in section 3.5 are considered; low density polyethylene (LDPE) , linear low density polyethylene (LLDPE), metallocene linear low density polyethylene (mLLDPE), Capilene SB56 , Buplen 6531, Petoplen MH-418 as polymers; LDPE-g-IA, LDPE-g-MMI, LLDPE-g-IA, LLDPE-g-MMI, mLLDPE-g-IA, PP-g-IA, as compatibilizers; DDA, HDA, and ODA modified montmorillonite, Nanofil 8 as organoclays are used in process, and resulting “l/t” values are given in groups in below tables.

Table 4.1: Calculated “l/t” values below 10

Polymeric Nanocomposites	l/t
LDPE-IA-O _{DDA} 5-C5	0.46
mLLDPE- O _{ODA} 5 - C 5	7.72
mLLDPE - O _{ODA} 5 - C 10	8.43
mLLDPE - O _{ODA} 5 - C 15	0.34
mLLDPE - O _{ODA} 5 - C 20	0.01
PP _{CAP} – O _{NANOFIL8} 3 – C10	0.01

Table 4.2: Calculated “l/t” values between 10 and 50

Polymeric Nanocomposites	l/t
LDPE- MMI-O _{DDA} 5-C5	31.73
LDPE- MMI-O _{HDA} 5-C5	44.44
LDPE-IA-O _{ODA} 5-C5	42.09
LDPE- MMI-O _{ODA} 5-C5	30.35
LLDPE – IA- O _{DDA} 5 – C5	31.55
LLDPE-MMI-O _{DDA} 5-C5	26.10
LLDPE-MMI-O _{DDA} 5-C10	42.90
LLDPE-IA-O _{HDA} 5-C5	26.91
LLDPE-IA-O _{HDA} 5-C10	40.92
LLDPE-MMI-O _{HDA} 5-C5	22.83
LLDPE-MMI-O _{HDA} 5-C10	37.92
LLDPE-MMI-O _{HDA} 5-C15	49.22
LLDPE-IA-O _{ODA} 5-C5	13.13
LLDPE-MMI-O _{ODA} 5-C5	13.13
LLDPE-MMI-O _{ODA} 5-C10	38.32

PP _{CAP} – O _{NANOFIL8} 5–C15	18.31
PP _{BUP} – O _{NANOFIL8} 3– C10	37.41
PP _{BUP} – O _{NANOFIL8} 5– C15	30.54
PP _{MH418} – O _{NANOFIL8} 3– C10	11.03
PP _{MH418} – O _{NANOFIL8} 5– C 15	11.77

Table 4.3: Calculated “1/t” values between 50 and 100.

Polymeric Nancomposites	1/t
LDPE-IA-O _{DDA} 5-C10	51.85
LDPE- MMI-O _{DDA} 5-C10	57.09
LDPE-IA-O _{DDA} 5-C15	54.59
LDPE- MMI-O _{DDA} 5-C10	57.09
LDPE- MMI-O _{DDA} 5-C15	82.82
LDPE-IA-O _{HDA} 5-C5	55.97
LDPE-IA-O _{HDA} 5-C10	83.11
LDPE- MMI-O _{HDA} 5-C10	67.12
LDPE-IA-O _{ODA} 5-C10	65.76
LDPE-IA-O _{ODA} 5-C15	82.94
LDPE- MMI-OC _{ODA} 5-C15	67.94
LLDPE-IA-ODDA 5-C10	56.93
LLDPE-IA-ODDA 5-C15	67.52
LLDPE-MMI-ODDA 5-C15	63.23
LLDPE-IA-OHDA 5-C15	50.79
LLDPE-MMI-O _{HDA} 5-C15	49.22
LLDPE-IA-O _{ODA} 5-C10	50.44
LLDPE-IA-O _{ODA} 5-C15	99.48

Table 4.4: Calculated “1/t” values upper than 100.

Polymeric Nancomposites	1/t
LDPE-IA-O _{HDA} 5-C15	128.18
LDPE- MMI-O _{HDA} 5-C15	115.88
LLDPE-MMI-O _{ODA} 5-C15	100.31

In some calculation, the intercalation can be obtained either experimental XRD results or Halpin Tsai approach “1/t” calculations. The experimental XRD results which give the d-spacing and the calculated “1/t” of the POs give a presumption of

nanocomposite structure. The results calculated “ l/t ” by Halpin Tsai models consistent for the experimental XRD values.

For some samples partial exfoliation leads to an appreciable increase in the elastic modulus of the nanocomposites and “ l/t ” values are higher than 100 for these samples while the complete exfoliation approaches to 200.

4.2. Calculation of Young Modulus Values of Different Types of Nanocomposites by Halpin Tsai Micromechanical Model

In graphs below, “ l/t ” are taken as 10, 50, 100, 200 respectively in Halpin Tsai formulas. LDPE, LLDPE, PP (Buplen); Nanofil 8 are used and their properties are taken from section 3. %1, %5, %10 Nanofil 8 content are used in calculations, and mass of taken compatibilizers are three times of organoclay content. Following figures are obtained.

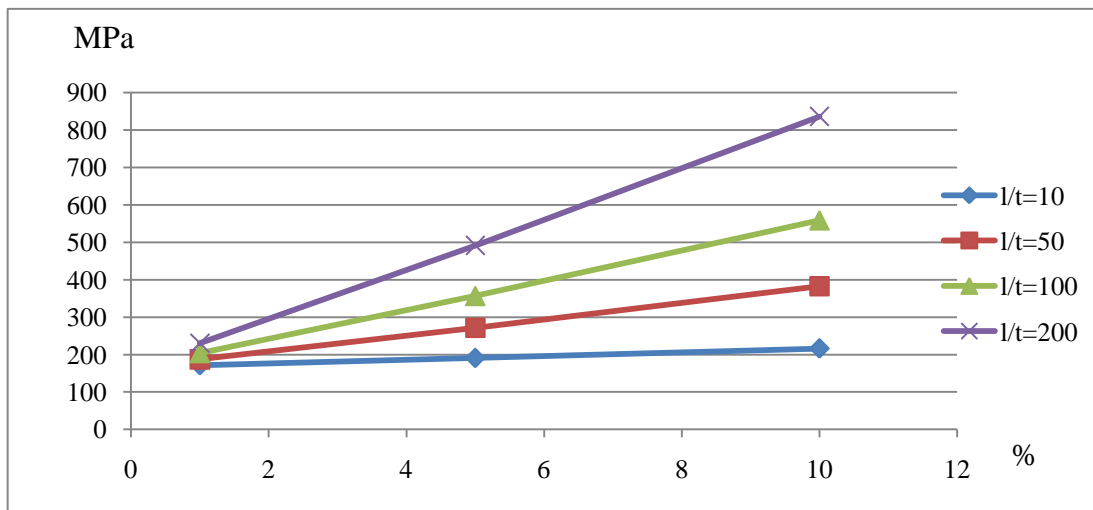


Figure 4.1 : Composite modulus versus Nanofil 8 content graph of LDPE

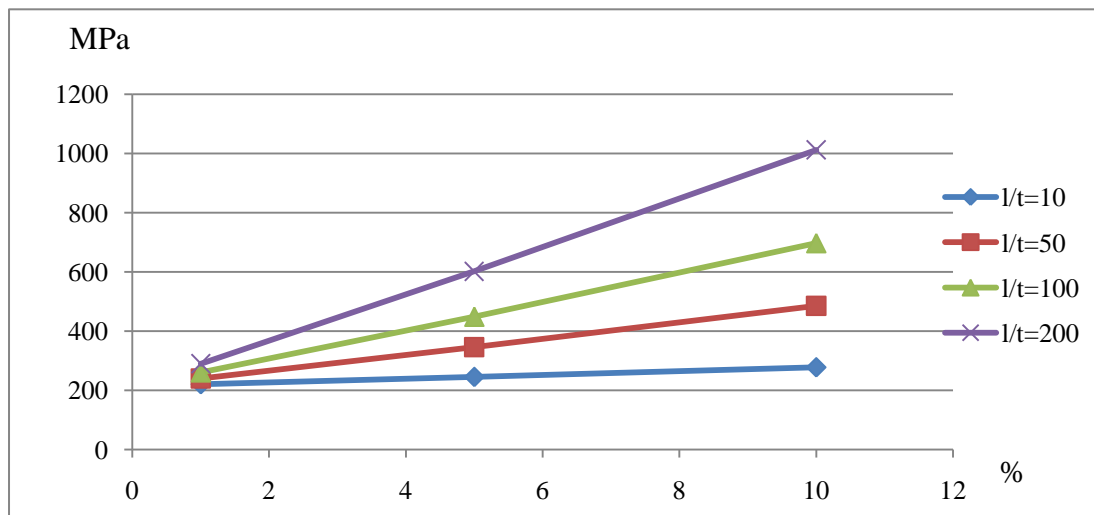


Figure 4.2 : Composite modulus versus Nanofil 8 content graph of LLDPE

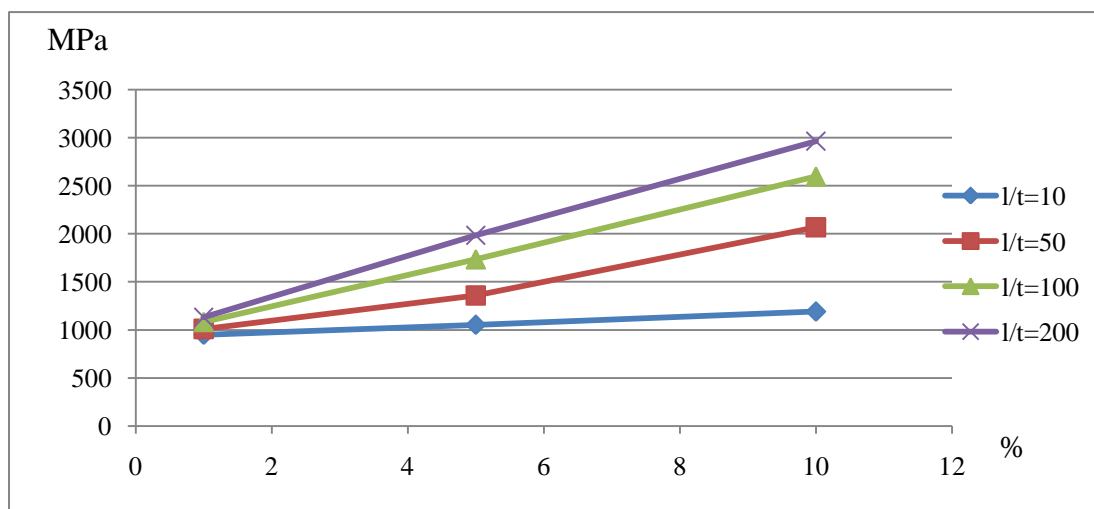


Figure 4.3 : Composite modulus versus Nanofil 8 content graph of PP (Buplen)

In above graphs “l/t” ratios change from 10 to 200. As “l/t” ratio rises, dispersion of layers increases in structure. This causes increment in Young modulus of polymeric nanocomposite. The higher content of organoclay, the higher elastic modulus of PNC.

It was observed that in graphs that, the slope of lines differ each other because of Young’s modulus differences of LDPE, LLDPE, PP (Buplen).

REFERENCES

- [1] **Utracki, L.A.**, 2004. Clay-Containing Polymeric Nanocomposites (vol. 2), Rapra Technology Ltd, Shropshire, UK. /Kim Y.c., Lee S.J., Kim J.C., Cho H., 2005. *Polym. J.*, 37, 1.
- [2] **Hasegawa, N., Kato M., Okamoto H., Tsukigase A., Usiki A.**, 2003. *Polym. Eng. Sci.*, **43**, 1312. / Lopez-Quintnilia M. L., Sanchez-Valdes S., Ramos de Vale L.F., Medellin-Rodriguez F.J., 2006. *J.Appl. Polym. Sci.*, **100**, 4748.
- [3] **Osman, M., A., Rupp, J., E., P., Suter, U., W.**, 2005. Tensile properties of polyethylene-layered silicate nanocomposites, *Polymer*, **46**, 5, 1653-1660
- [4] **Okada, A., Usuki, A.**, 2006. Twenty years of Polymer-Clay Nanocomposites, *Macromol. Mater. Eng.* , **291**: p. 1449–1476
- [5] **Chen, B., Evans, Julian, R., G.**, 2006. Elastic moduli of clay platelets, *Scripta Materialia*, **54**: p. 1581-1585.
- [6] **Harper, A., Charles**, 2004. *Handbook of plastics, elastomers, and composites*. 4 ed., The Mcgraw-hill companies, p. 52.
- [7] **Brydson, J., A.**, 1999. *Plastic materials, 7 ed: Butterworth Heinemann*, p. 251.
- [8] **Harper, A., Charles**, 2004. *Handbook of plastics, elastomers, and composites*. 4 ed., The McGraw-Hill Companies, p. 52.
- [9] **Brydson, J., A.**, 1999. *Plastic materials, 7 ed: Butterworth Heinemann*, p. 251.
- [10] **Karian, G., Harutun**, 2003. *Handbook of polypropylene and polypropylene composites*, 2 ed., Marcel Dekker Inc., p. 30.
- [11] **Calafut., T, Clive, M.**, 1998. *Polypropylene: The Definitive User's Guide and Databook*, William Andrew Inc
- [12] **Utracki, L. A.**, 1990. *Polymer Blends and Alloys*, New York,
- [13] **Walsh D. J.** 1985. *Polymer Blends and Mixtures*, NATO ASI Series E 89; Marinus Nijhoff: Boston
- [14] **Hasegawa, N., Kawasumi, M., Kato, M., Usuki, A., Okada, A.**, 1997. Preparation and Mechanical Properties of Polypropylene-Clay Hybrids, *Macromolecules*, Vol. **30**, No. 20.
- [15] **Alvarez, V., A., Bernal, C., R., Tarapow, J., A.**, *Journal of Appl. Polym. Sci.*, Vol. **111**, 768-778.
- [16] **Bhattacharya, S., N., Gupta, R., K., Kamal, M., R.**, 2008. *Polymeric Nanocomposites, Theory and Practice*, p.12.
- [17] **Rosoff, M.**, 2002. *Nano-Surface Chemistry*, p.653.
- [18] **Krishnamoorti, R., Vaia, R., A.**, 1996. Structure and dynamics of polymer-layered silicate nanocomposites. *Chemistry of Materials* **8**,1728.
- [19] **Burnside, S., D., Giannelis, E., P.**, 1995. Synthesis and properties of new poly(dimethylsiloxane) nanocomposites *Chem. Mater.*, 7 (9), 1597.

- [20] **Gilman J., W., Harris, R., Hilton D., Jackson, C., L., Morgan, A., B., Manias, E., Giannelis. E., M., Phillips, P., Wuthenow, S.,** 2000. Flammability Properties of Polymer – Layered - Silicate Nanocomposites. Polypropylene and Polystyrene Nanocomposites, *Chem. Mater.*, Vol.12, Iss.7, p.1866–1873
- [21] **Gupta, K.,R., Kennel, E., Kim,K., J.,** 2010. *Polymer Nanocomposites Handbook, Taylor and Francis Group*, p. 395
- [22] **Jia, Q., X., Wu, Y., P., Yu, D., S., Zhang LQ.,** 2004. Modeling Young’s modulus of rubber–clay nanocomposites using composite theories, *Polym Test*, **23**, 903–909.
- [23] **Bhattacharyya, D., Dong, Y.,** 2010. Mapping the real micro/nanostructures for the prediction of elastic moduli of polypropylene/clay nanocomposites, *Polymer* **51**, 816–824.
- [24] **Lu, G., Q., Yua, A., B., Zenga, Q., H.,** 2008. Multiscale modeling and simulation of polymer nanocomposites, *Prog. Polym. Sci.* **33**, 191–269
- [25] **Bhattacharyya, D., Y., Dong,** 2010. A simple micromechanical approach to predict mechanical behavior of polypropylene/organoclay nanocomposites based on representative volume element (RVE), *Computational Materials Science* **49**, 1–8.
- [26] **Yung, K., C., Wang, J., Yue, T., M.,** 2006. Modeling Young’s Modulus of Polymer layered Silicate Nanocomposites Using a Modified Halpin Tsai Micromechanical Model, *Journal of Reinforced Plastics and Composites*, **25**, 847.
- [27] **Şener., F,** 2008. *Preparation of Polymer Nanocomposites by Using Metallocene, Ms. Sc. Thesis, ITU.*
- [28] **Eriman, Bülent.,** 2008. *Effect of the Polyethylene Graft Copolymer to Structures and Mechanical Properties of Polyethylene/Clay Nanocomposites, Ms. Sc. Thesis, ITU.*
- [29] **Zorluca, M.,** 2010. *Polypropylene Nanocomposites: Preparation and Characterization Ms. Sc. Thesis, ITU.*
- [30] **Uyanık N., Erdem A.R., Can M.F., Çelik M.S.,** 2006. Epoxy nanocomposites curing by microwaves, *Polymer Eng. & Sci.*, **05**, 46, 385
- [31] **Marras, S., I.,** 2007. Thermal and colloidal behavior of amine-treated clays: The role of amphiphilic organic cation concentration, *Journal of Colloid and Interface Science* **315**, 520–527
- [32] **Hackman, I., Hollaway, L.,** 2006. Epoxy-layered silicate nanocomposites in civil engineering, *Composites: Part A* **37**, 1161–1170
- [33] **Nanofil® 8 Dataheet**
- [34] **Retuert, J., Quyada, R., Vega. H., Yazdani, M.,** 2003. Compatibilizers Based on Polypropylene Grafted With Itaconic Acid Derivatives. Effect on Polypropylene/Polyethylene Terephthalate Blends, *Polymer Engineering and Science*, Vol. **43**, No. 4
- [35] **Gronski, W., Privalko, V.,P., Ponomarenko, S.,M., Privalko, E., G., Schon, F.,** 2005. Thermoelasticity and stress relaxation behavior of polychloroprene/organoclay nanocomposites, *European Polymer Journal*, **41**, 3042–3050
- [36] **Acierno, D., Dintcheva, N., T., Filippone, G., Mantia, F.,P.,** 2006. The role of organoclay in promoting co-continuous morphology in high-density poly(ethylene)/poly(amide) 6 blends

- [32] **Burnside, S.,D., Giannelis, E., P., Hui, C., Y., Shia, D.,** 1998. An interface model for the prediction of Young's modulus of layered silicate elastomer nanocomposites. *Polym Composites*,**19**, 608–17
- [38] **Masenelli, K., Reynaud., E., Vigier, G., Varlet, J.,** 2002. Mechanical properties of clay-reinforced polyamide. *J Polym Sci: Part B: Polym Phys*, **40**, 272–83.
- [39] **Kornmann, X., Berglund, L., A., Sterte, J., Giannelis E., P.,** 1998. Nanocomposites based on montmorillonite and unsaturated polyester. *Polym Eng Sci*, **38**, 1351–8.
- [40] **J., Wang, R., Pyrz,** 2004. Prediction of the overall moduli of layered silicate-reinforced nanocomposites—part I: basic theory and formulas, *Composites Science and Technology*, *64*, 925–934
- [41] **Cloisite® 20A Datasheet**

CURRICULUM VITAE



Candidate's full name: Özay AKSOY

Place and date of birth: İZMİR/ 16.05.1980

Permanent Address: 1834 Sok. No: 34 D: 7 Karşıyaka / İZMİR

Universities attended: Mechanical Engineering Department / Istanbul
Technical University